

OBSERVATIONAL CONSTRAINTS ON THE DEPENDENCE OF RADIO-QUIET QUASAR X-RAY EMISSION ON BLACK HOLE MASS AND ACCRETION RATE

BRANDON C. KELLY, JILL BECHTOLD, JONATHAN R. TRUMP, MARIANNE VESTERGAARD¹
Steward Observatory, University of Arizona, 933 N Cherry Ave., Tucson, AZ 85710

AND

ANETA SIEMIGINOWSKA
Harvard-Smithsonian Center for Astrophysics, 60 Garden Street, Cambridge, MA 02138
Draft version November 7, 2018

ABSTRACT

In this work we use a sample of 318 radio-quiet quasars (RQQ) to investigate the dependence of the ratio of optical/UV flux to X-ray flux, α_{ox} , and the X-ray photon index, Γ_X , on black hole mass, UV luminosity relative to Eddington, and X-ray luminosity relative to Eddington. Our sample is drawn from the literature, with X-ray data from *ROSAT* and *Chandra*, and optical data mostly from the SDSS; 153 of these sources have estimates of Γ_X from *Chandra*. We estimate M_{BH} using standard estimates derived from the H β , Mg II, and C IV broad emission lines. Our sample spans a broad range in black hole mass ($10^6 \lesssim M_{\text{BH}}/M_{\odot} \lesssim 10^{10}$), redshift ($0 < z < 4.8$), and luminosity ($10^{43} \lesssim \lambda L_{\lambda}(2500\text{\AA})[\text{erg s}^{-1}] \lesssim 10^{48}$). We find that α_{ox} increases with increasing M_{BH} and $L_{\text{UV}}/L_{\text{Edd}}$, and decreases with increasing L_X/L_{Edd} . In addition, we confirm the correlation seen in previous studies between Γ_X and M_{BH} and both $L_{\text{UV}}/L_{\text{Edd}}$ and L_X/L_{Edd} ; however, we also find evidence that the dependence of Γ_X of these quantities is not monotonic, changing sign at $M_{\text{BH}} \sim 3 \times 10^8 M_{\odot}$. We argue that the α_{ox} correlations imply that the fraction of bolometric luminosity emitted by the accretion disk, as compared to the corona, increases with increasing accretion rate relative to Eddington, \dot{m} . In addition, we argue that the Γ_X trends are caused by a dependence of X-ray spectral index on \dot{m} . We discuss our results within the context of accretion models with comptonizing corona, and discuss the implications of the α_{ox} correlations for quasar feedback. To date, this is the largest study of the dependence of RQQ X-ray parameters on black hole mass and related quantities, and the first to attempt to correct for the large statistical uncertainty in the broad line mass estimates.

Subject headings: accretion disks — galaxies: active — quasars: general — ultraviolet: galaxies — X-rays: galaxies

1. INTRODUCTION

The extraordinary activity associated with quasars involves accretion onto a supermassive black hole (SMBH), with the UV/optical emission arising from a geometrically thin, optically thick cold accretion disk (Shakura & Syun'yaev 1973), and the X-ray continuum arising from a hot, optically thin corona that Compton upscatters the disk UV photons (e.g., Haardt & Maraschi 1991). In highly accreting objects, like quasars ($0.01 \lesssim L_{\text{bol}}/L_{\text{Edd}} \lesssim 1$, e.g., Woo & Urry 2002; Vestergaard 2004; McLure & Dunlop 2004; Kollmeier et al. 2006), the X-ray plasma geometry is expected to be that of a hot, possibly patchy, ionized ‘skin’ that sandwiches the cold disk (e.g., Bisnovatyi-Kogan & Blinnikov 1977; Liang & Price 1977; Nayakshin 2000). However, the evidence for this is not conclusive, and relies on data from X-ray binaries and low- z sources (e.g., see the discussion by Czerny et al. 2003). Other geometries are possible, including an accretion disk that evaporates into a hot inner flow (e.g., Shapiro et al. 1976; Zdziarski et al. 1999), or a combination of a hot inner flow and a corona that sandwiches the disk (e.g., Poutanen et al. 1997;

Sobolewska et al. 2004a). Furthermore, radiation pressure can drive an outflow from the disk into the corona if the two are cospatial, thus altering the physics of the corona (Proga 2005). Investigations of how quasar X-ray parameters depend on black hole mass, M_{BH} , and accretion rate relative to Eddington, \dot{m} , offer important constraints on models of the disk/corona system.

There have been attempts to link the evolution of SMBHs to analytic and semi-analytic models of structure formation (e.g., Kauffmann & Haehnelt 2000; Hatziminaoglou et al. 2003; Bromley et al. 2004), where black holes grow by accreting gas funneled towards the center during a galaxy merger until feedback energy from the SMBH expels gas and shuts off the accretion process (e.g., Silk & Rees 1998; Fabian 1999; Wyithe & Loeb 2003; Begelman & Nath 2005). This ‘self-regulated’ growth of black holes has recently been successfully applied in smoothed particle hydrodynamics simulations (Di Matteo et al. 2005; Springel et al. 2005). Within this framework, the AGN or quasar phase occurs during the episode of significant accretion that follows the galaxy merger, persisting until feedback from the black hole ‘blows’ the gas away (e.g., Hopkins et al. 2006). Hydrodynamic calculations have shown that line pressure is more efficient than thermal pressure at driving an outflow (Proga 2007), and therefore, the efficiency of AGN feedback depends on the fraction of energy emitted

Electronic address: bkelly@as.arizona.edu

¹ Dept. of Physics and Astronomy, Robinson Hall, Tufts University, Medford, MA 02155 (present address)

through the UV/disk component as compared to the X-ray/corona component. If the fraction of energy emitted in the UV as compared to the X-ray depends on M_{BH} or \dot{m} , then it follows that the efficiency of AGN feedback will also depend on M_{BH} and \dot{m} . This has important consequences for models of SMBH growth, as the SMBH may become more or less efficient at driving an outflow depending on its mass and accretion rate. Studies of the dependence of quasar X-ray/UV emission on black hole mass and accretion rate are therefore important as they allow us to constrain a M_{BH} - or \dot{m} -dependent feedback efficiency.

Numerous previous studies have searched for a luminosity and redshift dependence of $\alpha_{ox} = -0.384 \log L_X/L_{UV}$, the ratio of X-ray to UV/optical flux (e.g., Avni & Tananbaum 1982; Wilkes et al. 1994; Yuan et al. 1998; Vignali et al. 2003b; Strateva et al. 2005; Steffen et al. 2006; Kelly et al. 2007), and Γ_X , the X-ray spectra slope (e.g., Reeves & Turner 2000; Bechtold et al. 2003; Dai et al. 2004; Risaliti & Elvis 2005; Grupe et al. 2006). Most studies have found a correlation between α_{ox} and UV luminosity, L_{UV} , while the existence of a correlation between α_{ox} and z is still a matter of debate (e.g., Bechtold et al. 2003; Vignali et al. 2003b; Steffen et al. 2006; Just et al. 2007; Kelly et al. 2007). In addition, studies of Γ_X have produced mixed results. Some authors have claimed a correlation between Γ_X and luminosity (e.g., Bechtold et al. 2003; Dai et al. 2004) or redshift (e.g., Reeves et al. 1997; Vignali et al. 1999; Page et al. 2003), while, others find no evidence for a correlation between Γ_X and L_{UV} or z (e.g., Vignali et al. 2005; Risaliti & Elvis 2005; Kelly et al. 2007).

A correlation between Γ_X and the $FWHM$ of the $H\beta$ line has also been found (e.g., Boller et al. 1996; Brandt et al. 1997), suggesting a correlation between Γ_X and black hole mass or Eddington ratio (e.g., Laor et al. 1997; Brandt & Boller 1998). Recently, it has become possible to obtain estimates of M_{BH} for broad line AGN by calibrating results from reverberation mapping (Peterson et al. 2004; Kaspi et al. 2005) for use on single-epoch spectra (Wandel et al. 1999; Vestergaard 2002; McLure & Jarvis 2002; Vestergaard & Peterson 2006; Kelly & Bechtold 2007). This has enabled some authors to confirm a correlation between Γ_X and either M_{BH} or L_{bol}/L_{Edd} (e.g., Lu & Yu 1999; Gierliński & Done 2004; Porquet et al. 2004; Piconcelli et al. 2005; Shemmer et al. 2006), where the X-ray continuum hardens with increasing M_{BH} or softens with increasing L_{bol}/L_{Edd} . In addition, previous work has also found evidence for quasars becoming more X-ray quiet as M_{BH} or L_{bol}/L_{Edd} increase (Brunner et al. 1997; Wang et al. 2004); however, studies involving the dependence of α_{ox} on M_{BH} or L_{bol}/L_{Edd} have remained rare compared to studies of Γ_X . It is important to note that the correlations inferred in previous work generally employ broad line mass estimates in combination with a constant bolometric correction. Therefore, most of the correlations found in previous work are, strictly speaking, between Γ_X or α_{ox} and the estimates $M_{BH} \propto L_\lambda^\gamma FWHM^2$ and $L_{bol}/L_{Edd} \propto L_\lambda^{1-\gamma} FWHM^{-2}$, where $\gamma \sim 0.5$.

In this work, we investigate the dependence of α_{ox} and Γ_X on black hole mass, optical/UV luminosity relative to Eddington, and X-ray luminosity relative to Eddington. We combine the main Sloan Digital Sky Survey (SDSS) sample of Strateva et al. (2005) with the sample of Kelly et al. (2007), creating a sample of 318 radio-quiet quasars (RQQ) with X-ray data from *ROSAT* and *Chandra*, and optical spectra mostly from the SDSS; 153 of these sources have estimates of Γ_X from *Chandra*. Because the X-ray emission in radio-loud sources can have an additional component from the jet (e.g., Zamorani et al. 1981; Wilkes & Elvis 1987), we focus our analysis on the radio-quiet majority. Our sample has a detection fraction of 87% and spans a broad range in black hole mass ($10^6 \lesssim M_{BH}/M_\odot \lesssim 10^{10}$), redshift ($0 < z < 4.8$), and luminosity ($10^{43} \lesssim \lambda L_\lambda(2500\text{\AA})[\text{erg s}^{-1}] \lesssim 10^{48}$), enabling us to effectively look for trends regarding α_{ox} and Γ_X .

The outline of this paper is as follows. In § 2 we describe the construction of our sample, and in § 3 we describe the procedure we used to fit the optical continuum and emission lines. In § 4 we describe how we obtain broad line mass estimates, our bolometric correction, and argue that a constant bolometric correction provides a poor estimate of the bolometric luminosity. In § 5 we describe the results from a regression analysis of α_{ox} on $M_{BH}, L_{UV}/L_{Edd}$, and L_X/L_{Edd} , and in § 6 we report evidence for a non-monotonic dependence of Γ_X on either $M_{BH}, L_{UV}/L_{Edd}$, and L_X/L_{Edd} . In § 7 we discuss our results within the context of AGN disk/corona models, and we discuss the implications for a dependence of quasar feedback efficiency on black hole mass or accretion rate. In § 8 we summarize our main results.

We adopt a cosmology based on the the WMAP best-fit parameters ($h = 0.71, \Omega_m = 0.27, \Omega_\Lambda = 0.73$, Spergel et al. 2003). For ease of notation, we define $L_{UV} \equiv \nu L_\nu(2500\text{\AA}), L_X \equiv \nu L_\nu(2 \text{ keV}), l_{UV} \equiv \log \nu L_\nu(2500\text{\AA})$, and $m_{BH} \equiv \log M_{BH}/M_\odot$.

2. SAMPLE CONSTRUCTION

In this analysis we combine 169 RQQs from Kelly et al. (2007, hereafter K07) with 149 RQQs from the main SDSS sample of Strateva et al. (2005, hereafter S05) to create a sample of 318 RQQs. Out of these 318 sources, 276 (86.8%) are detected in the X-rays. The $z \lesssim 4$ sources from the K07 sample were selected by cross-correlating the SDSS DR3 quasar catalogue (Schneider et al. 2005) with the *Chandra* public archive as of 2005 February 22. The $z \gtrsim 4$ sources from the K07 sample consist of targeted *Chandra* RQQs taken from the literature (Bechtold et al. 2003; Vignali et al. 2001, 2003a), and new observations reported by K07. The sources taken from S05 were selected from the SDSS to be contained within the inner $19'$ of *ROSAT* PSPC pointings with exposure times > 11 ksec. The X-ray data for both samples are as reported by S05 and K07.

Both the S05 and K07 samples consist only of radio-quiet quasars. We focus our analysis on the radio-quiet majority because the radio-loud sources have an additional component of X-ray emission arising from the jet (e.g., Zamorani et al. 1981; Wilkes & Elvis 1987; Worrall et al. 1987). In addition, both S05 and K07 omitted BAL QSOs when possible. It is necessary to

remove the BAL QSOs because their high column density gives them the appearance of being X-ray weak (e.g., Green et al. 2001; Gallagher et al. 2002, 2006), potentially biasing our analysis. However, neither S05 nor K07 were able to remove the high-ionization BAL quasars for $z < 1.5$, as their identification requires observations of the C IV line. In addition, low-ionization BALs can be identified at $0.45 < z < 2.25$ based on Mg II absorption. Reichard et al. (2003) found the fraction of BALs in the SDSS to be $\sim 14\%$, and therefore we expect there to be 25 ± 5 BALs in our sample at $z < 1.5$. This number may be higher if one relaxes the definition of a BAL quasar (Trump et al. 2006).

We exclude five sources from the S05 sample due to significant intrinsic narrow UV absorption or obvious host galaxy contamination: Source SDSS J103747.4-001643.9 ($z = 1.500$) had significant C IV absorption, and sources SDSS J124520.7-002128.1 ($z = 2.354$) and SDSS J103709.8+000235.2 ($z = 2.679$) had significant absorption in both C IV and $L\alpha$. These three sources were omitted because the absorption prohibits obtaining an accurate line width measurement, necessary for broad line mass estimates, and to ensure that the X-ray emission under study is not effected by the absorption. Sources SDSS J230440.6-082220.8 ($z = 0.201$) and SDSS J023306.0+003856.4 ($z = 0.244$) have a significant host-galaxy component in their spectra. In addition, we exclude source SDSS J144340.8+585653.2 ($z = 4.278$) from the K07 sample because it has significant UV absorption. We removed source SDSS J142414.1+421400.1 ($z = 1.608$) from the K07 sample and source SDSS J170441.4+604430.5 (PG 1704+608, $z = 0.372$) from the S05 sample, as both sources are radio-loud.

We could not estimate black hole masses for sources SDSS J083206.0+524359.3 ($z = 1.573$), SDSS J144231.7+011055.3 ($z = 4.507$), and PC 0910+5625 ($z = 4.035$). All three of these sources are from the K07 sample. The region containing the Mg II emission line for SDSS J083206.0+524359.3 was missing from the SDSS spectrum, the emission lines are too weak for SDSS J144231.7+011055.3, and an optical spectrum was not available for PC 0910+5625.

3. OPTICAL/UV SPECTRAL FITS

Optical spectra were obtained for most sources from the SDSS. We also obtained spectra for some of the high redshift quasars from Anderson et al. (2001), Péroux et al. (2001), and Constantin et al. (2002). The values of L_{UV} and α , $L_\nu \propto \nu^{-\alpha}$, for the K07 sources are taken from K07. We processed the optical spectra for the S05 sources in the same manner as for the K07 sources. We do this for consistency and because S05 did not correct for quasar iron emission.

3.1. Continuum Fitting

As described by K07, we corrected the optical spectra for Galactic absorption using the $E(B - V)$ values taken from Schlegel et al. (1998), as listed in the NASA/IPAC Extragalactic Database (NED), and the extinction curve of Cardelli et al. (1989), assuming a value of $A_V/E(B - V) = 3.1$. We model the continuum as a power law of the form $f_\nu \propto \nu^{-\alpha}$, and the Fe emission as a scaled and broadened iron template extracted from I Zw 1. The optical iron template was extracted

by Véron-Cetty et al. (2004), and the UV iron template was extracted by Vestergaard & Wilkes (2001). The continuum and iron emission were fit simultaneously using the Levenberg-Marquardt method for nonlinear χ^2 -minimization. Continuum flux densities were then estimated using the power law parameters.

We were not able to use a power-law fit to calculate L_{UV} for the $z \lesssim 0.4$ sources, as the SDSS spectral range for these sources does not contain the rest-frame UV continuum. Instead, we use the luminosity of the broad component of the $H\beta$ emission line, $L_{H\beta}$, as a proxy for L_{UV} . It is preferable to use the broad $H\beta$ emission line luminosity over, say, the optical continuum luminosity as a proxy for L_{UV} because the broad $H\beta$ emission line is not contaminated by emission from the host galaxy, and thus should provide an approximately unbiased estimate of L_{UV} . Host-galaxy contamination is likely negligible for all $z > 0.4$ sources, as $\nu L_\nu^* \sim 10^{44}$ ergs s^{-1} at 2500\AA for galaxies (Budavári et al. 2005). We fit a power-law relationship between L_{UV} and $L_{H\beta}$ using the 44 sources at $0.4 < z < 0.9$ for which a measurement of both quantities is available. We used the linear regression method of Kelly (2007), which allows for measurement errors in both variables, and find

$$\frac{\lambda L_\lambda(2500\text{\AA})}{10^{44} \text{ ergs s}^{-1}} = (1.556 \pm 0.282) \left(\frac{L_{H\beta}}{10^{42} \text{ ergs s}^{-1}} \right)^{0.768 \pm 0.086} \quad (1)$$

The intrinsic scatter about this relationship is ≈ 0.179 dex, implying a potential uncertainty in L_{UV} inferred from this relationship of the same magnitude. There was no trend in the residuals with either z or $L_{H\beta}$, implying that Equation (1) should give unbiased estimates of L_{UV} for the $z < 0.4$ sources. Values of L_{UV} were estimated using Equation (1) for both the K07 and S05 $z < 0.4$ sources, a total of 42 sources.

The distributions of L_{UV} and L_X as a function of redshift are shown in Figure 1. We calculate the ratio of optical to X-ray flux (Tananbaum et al. 1979) as

$$\alpha_{ox} = -0.384 \log(f_{2\text{keV}}/f_{2500}), \quad (2)$$

where $f_{2\text{keV}}$ and f_{2500} are the rest-frame flux densities at 2 keV and 2500\AA , respectively. If the flux density from 2500\AA to 2 keV is a simple power law, then α_{ox} is the spectral slope of this continuum, and thus α_{ox} may be thought of as a crude estimate of the shape of the ionizing continuum. The parameter α_{ox} is an important parameter for model comparison, as it summarizes the amount of energy emitted in the X-ray region (most likely a Comptonized component), compared with that emitted in the optical-UV (accretion disk component). The distribution of α_{ox} as a function of L_{UV} and z are also shown in Figure 1.

The error on α_{ox} is the result of measurement errors on the UV and X-ray flux, as well as error caused by quasar variability over the different epochs for the UV and X-ray observations. In general, the measurement errors on L_{UV} are negligible compared to the error on L_X . S05 estimates a error on the X-ray flux of ~ 0.23 dex, including both the contributions from measurement error and variability. Typical long-term X-ray variability for Seyfert 1s is 20%–40% with no obvious trend with luminosity (Grupe et al. 2001; Uttley et al. 2002; Markowitz et al.

2003). The measurement errors in l_X for the K07 sample are typically ~ 0.07 dex. Assuming X-ray variability amplitudes of 30%, this implies typical uncertainties in the X-ray luminosity of ~ 0.15 dex. Therefore, we estimate the uncertainty on α_{ox} to be ~ 0.06 for the K07 sources and ~ 0.09 for the S05 sources.

3.2. Line Profile Extraction and Fitting

We extracted the H β , Mg II, and C IV emission lines in order to use their widths in our black hole mass estimates (e.g., Vestergaard 2002; McLure & Jarvis 2002; Vestergaard & Peterson 2006). These lines were extracted by first subtracting the continuum and Fe emission, interpolating over any narrow absorption features, and modelling all lines within the extraction region as a sum of Gaussian functions. Any nearby lines were then subtracted, leaving only the broad emission line profile. In all cases the line profile extraction was done interactively and every line fit was inspected visually.

For H β , we extracted the region within $\pm 2 \times 10^4 \text{ km s}^{-1}$ of 4861\AA , where we use the standard convention that negative velocities are blueward of a given wavelength. The H β profile was modeled as a sum of 2–3 Gaussian functions. The [O III] $\lambda 4959\text{\AA}$ and [O III] $\lambda 5007\text{\AA}$ lines were modeled as a sum of 1–2 Gaussian functions, depending on the signal-to-noise of the lines. A sum of two Gaussian functions was used for the higher S/N lines because the [O III] line profiles are not exactly a Gaussian function; the individual Gaussian components are not considered to be physically distinct components. The widths of the narrow Gaussian functions for H β and [O III] lines were fixed to be equal to each other. The [O III] lines and the narrow component of the H β line were then subtracted, leaving the broad component of H β .

For Mg II, we extracted the region within $\pm 2 \times 10^4 \text{ km s}^{-1}$ of 2800\AA . There are no nearby non-iron emission lines that Mg II is blended with, so the extraction is trivial after removing the Fe and continuum emission.

For C IV, we extracted the region within $-2 \times 10^4 \text{ km s}^{-1}$ and $3 \times 10^4 \text{ km s}^{-1}$ of 1549\AA . The C IV line was modeled as a sum of 2–3 Gaussian functions, and He II $\lambda 1640$ and O III] $\lambda 1665$ were modeled as a sum of 1–2 Gaussian functions each. After obtaining estimates of the He II and O III] profiles, we subtracted these components. We did not model the N IV] $\lambda 1486$ emission line as this line is typically weak and lost in the C IV wings.

In order to estimate M_{BH} , it is necessary to measure the $FWHM$ of the emission lines. After extracting the line profiles, we estimate the $FWHM$ for the H β , Mg II, and C IV emission lines by fitting them to a sum of 1–5 Gaussian functions, enabling us to obtain a smooth representation of each line. In contrast to our profile extraction technique, we choose the number of Gaussian functions to minimize the Bayesian Information Criterion (BIC , Schwartz 1979). The BIC is a common criterion to use for selecting the number of parameters in a model (e.g., see Hastie, Tibshirani, & Friedman 2001); the model that minimizes the BIC is approximately the model that is most supported by the data. For Gaussian errors, as assumed in this work, the BIC is simply a

modification to the standard χ^2 statistic:

$$BIC = \chi^2 + 3K \ln n, \quad (3)$$

where K is the number of Gaussian functions used, $3K$ is the number of free parameters, and n is the number of data points used in the fit. Using the BIC to ‘fit’ the number of Gaussian functions thus allows us more flexibility in obtaining a smooth representation of the line profile, as we are not choosing the number of Gaussian functions arbitrarily. Once a smooth representation is obtained, we automatically measure the $FWHM$ directly from the best fit line profile.

The standard errors on $FWHM$ are estimated using a bootstrap method. We simulated 100 ‘observed’ emission lines by adding random Gaussian noise to the best fit line profile with standard deviation equal to the noise level of the spectrum, including the propagated errors from the continuum and iron emission fitting. We then fit each of the simulated emission lines, keeping the number of Gaussian functions fixed at the number found from fitting the original profile, and measured the $FWHM$ for each simulated line. The standard error on $FWHM$ was then estimated as the standard deviation of the $FWHM$ values measured from the simulated line profiles.

4. ESTIMATING M_{BH}

Recently, reverberation mapping studies of broad line AGN (e.g., Peterson et al. 2004) established a correlation between the broad line region (BLR) size, R , and the continuum luminosity (the R – L relationship, e.g., Kaspi et al. 2005; Bentz et al. 2006). This has made it possible to estimate black hole virial mass $M_{BH} = fv^2R/G$ for individual sources, where the BLR velocity v is estimated from the width of an emission line (e.g., Wandel et al. 1999; Vestergaard 2002; McLure & Jarvis 2002; Vestergaard & Peterson 2006). We choose the proportionality constant to give broad line mass estimates consistent with the M_{BH} – σ relationship (Gebhardt et al. 2000; Merritt & Ferrarese 2001; Tremaine et al. 2002), $f = 1.4 \pm 0.45$ (Onken et al. 2004). An estimate of the Eddington luminosity can be computed as $L_{Edd} = 1.3 \times 10^{38} M_{BH}/M_{\odot} \text{ erg s}^{-1}$.

4.1. Black Hole Mass Estimates from H β , Mg II, and C IV

In this work we estimate M_{BH} from the H β , Mg II, and C IV emission lines. We use the relationship of Vestergaard & Peterson (2006) to estimate M_{BH} from the H β and C IV emission lines, and the details of the Mg II calibration will be discussed in a forthcoming paper Vestergaard et al. (2008, in preparation). The calibration for the Mg II mass estimates was calculated to ensure that they are consistent with the mass estimates based on H β and C IV. We have 49 sources with both H β and Mg II mass estimates, and 73 sources with both C IV and Mg II mass estimates. Both samples show consistent mass estimates between the different emission lines, within the intrinsic uncertainty in the broad line mass estimates (~ 0.4 dex).

We will denote the broad line mass estimates as \hat{M}_{BL} , and $\hat{m}_{BL} \equiv \log \hat{M}_{BL}/M_{\odot}$. It is important to distinguish between \hat{M}_{BL} and M_{BH} , as $\hat{M}_{BL} \propto L^{\gamma} FWHM^2$, $\gamma \sim 0.5$, is an estimate of M_{BH} derived from reverberation

mapping, and thus in general $\hat{M}_{BL} \neq M_{BH}$. The statistical uncertainty needs to be taken into account when analyzing correlations involving derived quantities like $\hat{M}_{BL} \propto L^\gamma FWHM^2$, as they can bias the results (Kelly & Bechtold 2007; Kelly 2007).

The uncertainty in f increases the formal statistical uncertainty in the broad line estimates of M_{BH} to ~ 0.46 dex. Our adopted formal uncertainty of ~ 0.46 dex is merely statistical, and additional systematic uncertainties in reverberation mapping may contribute (Krolik 2001; Collin et al. 2006). Because our adopted uncertainty of ~ 0.46 describes the scatter in broad line mass estimates about the reverberation mapping estimates, as calibrated via the M_{BH} - σ relationship, the regression results found in this work should be understood as results that could have been obtained if we had reverberation-based M_{BH} for the sources in this work. However, instead of reverberation-based mass estimates, we have broad line mass estimates with ‘measurement error’ equal to ~ 0.46 dex with respect to the reverberation-based mass estimates, thus increasing the uncertainty from the regression analysis.

For most sources, measurement errors on $FWHM$ and L_λ did not significantly contribute to the uncertainty on M_{BH} . If there were two emission lines in the same spectrum we averaged the two mass estimates, where the average was weighted by the uncertainties in the two estimates. The distribution of M_{BH} as a function of z for our sample is shown in Figure 2. The broad line mass estimates for the sources in our sample are reported in Table 1.

4.2. Eddington Ratio Estimates

A constant bolometric correction has been used in most previous studies involving the AGN Eddington ratio. However, recent work by Vasudevan & Fabian (2007) has suggested that bolometric corrections show a large spread with no obvious dependence on luminosity. Furthermore, these authors found evidence that the bolometric correction depends on the Eddington ratio. This implies that the error in the bolometric correction is correlated with Eddington ratio, which therefore implies that the error in the estimated Eddington ratio is correlated with the actual Eddington ratio. An Eddington ratio-dependent error in the bolometric correction may cause problems when using the estimated Eddington ratios to infer correlations.

Further difficulties with a constant bolometric correction are illustrated with Figure 3. In 3 we plot α_{ox} as a function of L_{UV}/\hat{L}_{Edd} and L_X/\hat{L}_{Edd} , where we estimate the Eddington luminosity from the broad line mass estimates as $\hat{L}_{Edd} = 1.3 \times 10^{38} \hat{M}_{BL}/M_\odot \text{ erg s}^{-1}$. As with \hat{M}_{BL} , we use the notation \hat{L}_{Edd} to emphasize that \hat{L}_{Edd} is an estimate of the true L_{Edd} based on the broad line mass estimates, and therefore $\hat{L}_{Edd} \propto L^\gamma FWHM^2$. Constant bolometric corrections are often applied to either the optical/UV or X-ray luminosity. If a constant bolometric correction was valid for both L_{UV} and L_X , then we would expect that $L_{UV}/\hat{L}_{Edd} \propto L_X/\hat{L}_{Edd} \propto L_{bol}/L_{Edd}$. However, while a correlation between α_{ox} and both L_{UV}/\hat{L}_{Edd} and L_X/\hat{L}_{Edd} is apparent, they are of opposite sign. Because the correlations are of

opposite sign, it cannot be true that both L_{UV}/\hat{L}_{Edd} and L_X/\hat{L}_{Edd} are proportional to the Eddington ratio, L_{bol}/L_{Edd} .

Because of the current significant uncertainty regarding RQQ bolometric corrections, we take the conservative approach and merely compare α_{ox} and Γ_X with L_{UV}/L_{Edd} and L_X/L_{Edd} . The estimated values of L_{UV}/L_{Edd} and L_X/L_{Edd} for the sources in our sample are reported in Table 1. We can write $L_{UV}/L_{Edd} \propto f_{UV} L_{bol}/L_{Edd}$ and $L_X/L_{Edd} \propto f_X L_{bol}/L_{Edd}$, where f_{UV} and f_X are the inverses of the bolometric corrections for L_{UV} and L_X , respectively. The quantities f_{UV} and f_X are proportional to the fraction of the bolometric luminosity emitted at 2500Å and 2 keV. Then, correlations between either α_{ox} or Γ_X and L_{UV}/L_{Edd} will result if α_{ox} or Γ_X is correlated with f_{UV} , the Eddington ratio, or both, and likewise for f_X .

While we do not use an estimate of the Eddington ratio in our analysis, it is helpful to estimate the distribution of Eddington ratios probed by our sample. We assume the bolometric correction described in Hopkins et al. (2007) for the $z < 1.5$ sources, and constant bolometric described in Vestergaard (2004) of $L_{bol} = 4.62\lambda L_\lambda (1350\text{Å})$ at $z > 1.5$. In Figure 2 we also show the distribution of estimated Eddington ratios as a function of z . Because the distribution of estimated L_{bol}/L_{Edd} is the true distribution of L_{bol}/L_{Edd} broadened by the distribution of errors in the estimates, our sample likely probes a smaller range in Eddington ratio than that inferred from Figure 2. Therefore, at most our sample probes RQQs with Eddington ratios $0.03 \lesssim L_{bol}/L_{Edd} \lesssim 2$.

5. DEPENDENCE OF α_{OX} ON M_{BH} , L_{UV}/L_{EDD} , AND L_X/L_{EDD}

We used our sample of 318 sources with estimates of M_{BH} to investigate the dependence of α_{ox} at a given black hole mass, L_{UV}/L_{Edd} , and L_X/L_{Edd} . We use linear regression analysis in order to understand how α_{ox} varies with respect to these parameters. We use the method of Kelly (2007) to estimate the regression parameters. The method of Kelly (2007) accounts for measurement errors, non-detections, and intrinsic scatter. In addition, Kelly (2007) adopts a Bayesian approach, computing the posterior probability distribution of the parameters, given the observed data. Thus the uncertainties on the regression coefficients have a straightforward interpretation, and do not rely on large-sample approximations. Many other methods, such as traditional maximum-likelihood, assume that the errors in the regression parameters follow a Gaussian distribution, which is valid as the sample size approaches infinity. However, this assumption is not necessarily valid for our finite sample size, especially in the presence of censoring (i.e., presence of upper/lower limits) and significant measurement error. The method of Kelly (2007) directly estimates the probability distribution of the regression parameters, and is therefore preferred.

We assess the simple 2-dimensional correlations between α_{ox} and M_{BH} , L_{UV}/L_{Edd} , and L_X/L_{Edd} , and compare with the α_{ox} - L_{UV} correlation. The results from the regressions are

$$\alpha_{\text{ox}} = -3.91_{-1.01}^{+1.04} + (0.12_{-0.02}^{+0.02}) \log L_{UV}, \quad \sigma_{\alpha_{\text{ox}}} = 0.14_{-0.01}^{+0.02},$$

$$\begin{aligned} \rho &= 0.57^{+0.09}_{-0.10} \\ \alpha_{\text{ox}} &= 0.05^{+0.39}_{-0.42} + (0.17^{+0.05}_{-0.04}) \log M_{BH}, \quad \sigma_{\alpha_{\text{ox}}} = 0.14^{+0.02}_{-0.02}, \\ \rho &= 0.53^{+0.12}_{-0.13} \\ \alpha_{\text{ox}} &= 2.90^{+0.71}_{-0.43} + (0.99^{+0.50}_{-0.31}) \log L_{UV}/L_{Edd}, \quad \sigma_{\alpha_{\text{ox}}} = 0.05^{+0.05}_{-0.03}, \\ \rho &= 0.95^{+0.04}_{-0.16} \\ \alpha_{\text{ox}} &= -0.03^{+0.25}_{-0.34} - (0.57^{+0.09}_{-0.12}) \log L_X/L_{Edd}, \quad \sigma_{\alpha_{\text{ox}}} = 0.03^{+0.04}_{-0.03}, \\ \rho &= -0.98^{+0.06}_{-0.02} \end{aligned} \quad \begin{aligned} (4) \frac{L_\nu(2500\text{\AA})}{L_\nu(2\text{ keV})} &= 9.81^{+0.65}_{-0.63} \times 10^3 \left(\frac{M_{BH}}{10^9 M_\odot} \right)^{0.43 \pm 0.06}, \quad (9) \\ (5) \frac{L_\nu(2500\text{\AA})}{L_\nu(2\text{ keV})} &= 3.51^{+15.6}_{-2.58} \times 10^7 \left(\frac{\nu L_\nu(2500\text{\AA})}{L_{Edd}} \right)^{2.57 \pm 0.45}, \quad (10) \\ (6) \frac{L_\nu(2500\text{\AA})}{L_\nu(2\text{ keV})} &= 0.85^{+1.02}_{-0.52} \left(\frac{\nu L_\nu(2\text{ keV})}{L_{Edd}} \right)^{-1.48 \pm 0.14}, \quad (11) \end{aligned}$$

where $\sigma_{\alpha_{\text{ox}}}$ is the intrinsic dispersion in α_{ox} at a given L_{UV} , M_{BH} , L_{UV}/L_{Edd} , or L_X/L_{Edd} , ρ is the linear correlation coefficient for α_{ox} and the respective independent variables, and the errors are quoted at the 95% (2σ) level. All four relationships are significant, with RQQs becoming more X-ray quiet as L_{UV} , M_{BH} , or L_{UV}/L_{Edd} increases, and more X-ray loud as L_X/L_{Edd} increases. Because we have attempted to correct for the intrinsic statistical scatter in the broad line mass estimates, Equations (4)–(7) refer to the intrinsic relationships involving M_{BH} , barring any systematic errors in reverberation mapping, and are not simply correlations between α_{ox} and the broad line mass estimates. The estimated distributions of α_{ox} as a function of L_{UV} , M_{BH} , L_{UV}/L_{Edd} , and L_X/L_{Edd} are shown in Figure 4, along with the regression results.

The intrinsic dispersion in α_{ox} quantifies the magnitude of scatter in α_{ox} at a given L_{UV} , M_{BH} , L_{UV}/L_{Edd} , or L_X/L_{Edd} . Because we have attempted to account for contribution to the scatter in α_{ox} resulting from measurement error and variability, $\sigma_{\alpha_{\text{ox}}}$ represents the dispersion in the real physical scatter in α_{ox} over the population of RQQs. This ‘residual’ scatter represents the amount of variation in α_{ox} that is not ‘explained’ by variations in L_{UV} , M_{BH} , L_{UV}/L_{Edd} , or L_X/L_{Edd} , respectively. This intrinsic scatter in α_{ox} may be due to variations in accretion rate, viscosity, column density, and other quantities not included in our regression.

In § 2 we estimate that there are 25 ± 5 BAL quasars in our sample at $z < 1.5$. Because these objects have the appearance of being X-ray weak, and because redshift is artificially correlated with luminosity and M_{BH} in a flux limited sample, we expect that the presence of unidentified BALs at $z < 1.5$ will produce an excess of X-ray weak objects at low L_{UV} and M_{BH} , thus flattening the inferred slopes. Inspection of the plot of α_{ox} and z in Figure 1 suggests an excess of X-ray weak objects at $z < 1.5$ and $\alpha_{\text{ox}} \gtrsim 1.8$, implying these objects are BAL quasars. We removed these 10 objects and refit the regressions. Omission of these objects resulted in a steepening of the slopes for the L_{UV} and M_{BH} regression, and a flattening of the slope for the L_{UV}/L_{Edd} regression. In addition, the intrinsic dispersion in α_{ox} decreased for the L_{UV} and M_{BH} regressions, while it remained the same for the L_{UV}/L_{Edd} regression. These changes were small ($\sim 10\%$) and have no effect on our conclusions. There was no difference in the results for the L_X/L_{Edd} regression.

Once can use Equation (2) to express the regression results (Eq. [4]–[7]) in the alternate form

$$\frac{L_\nu(2500\text{\AA})}{L_\nu(2\text{ keV})} = 1.17^{+0.08}_{-0.07} \times 10^4 \left(\frac{\nu L_\nu(2500\text{\AA})}{10^{46} \text{ergs}^{-1}} \right)^{0.31 \pm 0.03} \quad (8)$$

where the intrinsic dispersion in $\log L_{UV}/L_X$ at a given L_{UV} , M_{BH} , L_{UV}/L_{Edd} , and L_X/L_{Edd} is $\sim 0.356, 0.375, 0.133$, and 0.089 dex, respectively. In contrast to Equations (4)–(7), we quote the 68% (1σ) uncertainties on the constants of proportionality, and the posterior standard deviations on the exponents. Equations (8)–(11) may be more physically interpretable and allow easier comparison with models.

6. NONMONOTONIC DEPENDENCE OF Γ_X , L_{UV}/L_{Edd} , AND L_X/L_{BOL}

Recent work has suggested a correlation between quasar X-ray spectral slope, $\alpha_X = \Gamma_X - 1$, $f_\nu \propto \nu^{-\alpha_X}$, and quasar Eddington ratio as inferred from broad line mass estimates based on the H β emission line (e.g., Porquet et al. 2004; Piconcelli et al. 2005; Shemmer et al. 2006). The Kelly et al. (2007) sample contains measurements of Γ_X for 157 sources, and we were able to estimate black hole masses for 153 of them. In this section we use these 153 RQQs to investigate the dependence of Γ_X on M_{BH} , L_{UV}/L_{Edd} , and L_X/L_{Edd} .

6.1. Regression Analysis

The distributions of Γ_X as a function of estimated black hole mass, L_{UV}/L_{Edd} , and L_X/L_{Edd} are shown in Figure 6 for the entire sample, and in Figure 7 separately for each emission line. While there does not appear to be a monotonic trend between Γ_X and M_{BH} , L_{UV}/L_{Edd} , or L_X/L_{Edd} when using the entire sample, there is evidence for a trend between Γ_X and these quantities when using the H β line, and an opposite trend between Γ_X and these quantities when using the C IV line.

We performed a linear regression of Γ_X on $\log M_{BH}$, $\log L_{UV}/L_{Edd}$, and $\log L_X/L_{Edd}$ separately for each emission line. As before, we used the method of Kelly (2007) when performing the regression in order to correct for the intrinsic statistical uncertainty in the broad line estimates of M_{BH} . The results for M_{BH} are

$$\Gamma_X = 5.69^{+7.32}_{-4.29} - (0.44^{+0.53}_{-0.91}) \log M_{BH}, \quad \sigma = 0.43^{+0.17}_{-0.17},$$

$$\rho = -0.45^{+0.53}_{-0.44}, \quad (\text{H}\beta) \quad (12)$$

$$\Gamma_X = -19.0^{+46.0}_{-68.0} - (1.92^{+7.73}_{-5.18}) \log M_{BH}, \quad \sigma = 0.27^{+0.12}_{-0.20},$$

$$\rho = -0.62^{+1.23}_{-0.36}, \quad (\text{MgII}) \quad (13)$$

$$\Gamma_X = -2.79^{+5.22}_{-10.8} + (0.52^{+1.17}_{-0.56}) \log M_{BH}, \quad \sigma = 0.22^{+0.11}_{-0.14},$$

$$\rho = 0.53^{+0.42}_{-0.58}, \quad (\text{CIV}) \quad (14)$$

the results for L_{UV}/L_{Edd} are

$$\Gamma_X = 3.96^{+2.28}_{-1.15} + (1.23^{+1.48}_{-0.75}) \log L_{UV}/L_{Edd}, \quad \sigma = 0.26^{+0.23}_{-0.21},$$

$$\rho = 0.87^{+0.13}_{-0.50}, \quad (\text{H}\beta) \quad (15)$$

$$\Gamma_X = 5.13^{+10.8}_{-14.4} + (2.14^{+7.28}_{-9.94}) \log L_{UV}/L_{Edd}, \quad \sigma = 0.28^{+0.12}_{-0.22},$$

$$\rho = 0.54^{+0.44}_{-1.40}, \quad (\text{MgII}) \quad (16)$$

$$\Gamma_X = 0.85_{-2.00}^{+0.78} - (0.95_{-1.69}^{+0.65}) \log L_{UV}/L_{Edd}, \quad \sigma = 0.17_{-0.13}^{+0.13},$$

$$\rho = -0.81_{-0.18}^{+0.53}, \quad (\text{CIV}) \quad (17)$$

and the results for L_X/L_{Edd} are

$$\Gamma_X = 4.24_{-1.43}^{+2.58} + (0.85_{-0.56}^{+1.01}) \log L_X/L_{Edd}, \quad \sigma = 0.33_{-0.21}^{+0.19},$$

$$\rho = 0.76_{-0.46}^{+0.22}, \quad (\text{H}\beta) \quad (18)$$

$$\Gamma_X = 7.26_{-7.13}^{+16.2} + (1.97_{-2.71}^{+5.96}) \log L_X/L_{Edd}, \quad \sigma = 0.23_{-0.18}^{+0.15},$$

$$\rho = 0.77_{-0.90}^{+0.22}, \quad (\text{MgII}) \quad (19)$$

$$\Gamma_X = -0.54_{-5.69}^{+4.05} - (0.96_{-2.17}^{+1.52}) \log L_X/L_{Edd}, \quad \sigma = 0.21_{-0.15}^{+0.13},$$

$$\rho = -0.65_{-0.34}^{+0.90} (\text{CIV}). \quad (20)$$

In these equations we have quoted the errors at 95% (2σ) confidence. The probability distributions of the slope and intrinsic dispersion are shown in Figure 8. The larger uncertainty in the results for the Mg II sample is likely caused by the more narrow range in L_{UV} , L_X , and M_{BH} probed.

There are formally no significant linear correlations for the Γ_X - M_{BH} relationship. However, there is a statistically significant difference between the H β and C IV slopes, with $\approx 99.3\%$ of the posterior probability at $\beta_m^{\text{CIV}} > \beta_m^{\text{H}\beta}$, where β_m denotes the Γ_X - $\log M_{BH}$ regression slope. The probability distribution for the difference in slopes from the M_{BH} regression is shown in Figure 9. The significant difference in the slope for the H β and C IV sample implies a nonlinear relationship between Γ_X and m_{BH} , in spite of the fact that the H β and C IV correlations themselves are not ‘statistically significant’. Results similar to the Γ_X - $\log M_{BH}$ regressions were found for the Γ_X - L_{UV}/L_{Edd} and Γ_X - L_X/L_{UV} regressions, but with opposite sign and higher statistical significance.

We performed monte carlo simulations as a consistency check on our inferred non-monotonicity of the Γ_X relationships. While we have attempted to account for the significant statistical uncertainty on the broad line mass estimates, we employ these monte carlo simulations to ensure that the observed non-monotonic behavior is not a spurious result caused by the uncertainty on M_{BH} . We performed 10^5 simulations under two null hypotheses: (1) that Γ_X is independent of L_{UV}/L_{Edd} , and (2) that Γ_X depends linearly on $\log L_{UV}/L_{Edd}$. For both cases we simulated black hole mass estimates derived from H β and C IV separately. We first simulated ‘true’ values of M_{BH} for each emission line from a normal distribution with means equal to the observed mean of the two respective subsamples, and variances equal to the difference between the observed variance of the subsamples and the average intrinsic variance in the broad line mass estimates. To simulate the uncertainty in the mass estimates, we added random Gaussian errors to these ‘true’ values of M_{BH} with standard deviation equal to the uncertainty in the mass estimates, ~ 0.4 dex. For the case where Γ_X was assumed to be independent of L_{UV}/L_{Edd} , we simulated values of Γ_X from a normal distribution with mean equal to the sample mean of Γ_X and variance equal to the difference between the observed variance in Γ_X and the average of the variance in the measurement errors. For the case where Γ_X was assumed to depend linearly on $\log L_{UV}/L_{Edd}$, we simulated values of Γ_X according to our best fit relationship to the H β subsample,

given by Equation (15). Finally, for both cases we added random Gaussian errors to the simulated values of Γ_X by randomly reshuffling the dispersions in the measurement errors in Γ_X .

For each of the 10^5 simulated samples, we selected those samples that displayed a non-monotonic trend, i.e., those sample where the slope for the H β -based regression had a different sign from the slope of the C IV-based regression. Under the hypothesis that Γ_X is independent of L_{UV}/L_{Edd} , only 3 of the 10^5 simulated samples had both a non-monotonic trend and an absolute value of the difference in slopes between the H β and C IV regression that were larger than that observed for our actual sample. Under the hypothesis that Γ_X depends linearly on $\log L_{UV}/L_{Edd}$, none of the 10^5 simulated samples exhibited a non-monotonic trend. Therefore, the observed non-monotonic trend in Γ_X with Eddington ratio is not a spurious result caused by the statistical uncertainty in the broad line mass estimates, in agreement with our Bayesian regression results.

In order to investigate whether the non-monotonicity in the dependence of Γ_X on Eddington ratio depends on M_{BH} , we performed a linear regression of Γ_X simultaneously on $\log L_{UV}/L_{Edd}$ and $\log M_{BH}$. This also allows us to quantify whether the Eddington ratio is the driver behind the Γ_X - M_{BH} relationship. In particular, the Γ_X - M_{BH} relationship is weak compared to the Eddington ratio relationships, and therefore it is reasonable to conclude that Eddington ratio is the primary driver in these relationships. We applied the multiple regression technique of Kelly (2007) separately to both the H β and C IV subsamples. The results are:

$$\Gamma_X = 2.58_{-3.80}^{+4.81} + (0.18_{-0.61}^{+0.60}) \log M_{BH} +$$

$$(1.32_{-0.80}^{+1.45}) \log L_{UV}/L_{Edd}, \quad \sigma = 0.28_{-0.22}^{+0.22}, \quad (\text{H}\beta) \quad (21)$$

$$\Gamma_X = -4.26_{-15.6}^{+6.45} + (0.56_{-0.61}^{+1.44}) \log M_{BH} -$$

$$(0.84_{-2.16}^{+0.75}) \log L_{UV}/L_{Edd}, \quad \sigma = 0.17_{-0.14}^{+0.14}, \quad (\text{CIV}) \quad (22)$$

Here, we have quoted the errors at 95% significance. There is no statistically significant evidence that Γ_X depends on M_{BH} at a given L_{UV}/L_{Edd} , and therefore we conclude that the primary driver in the Γ_X relationships is Eddington ratio. However, this does not rule out the possibility that the non-monotonic trends with Eddington ratio are the result of a discontinuous change in the slopes at a ‘critical’ M_{BH} , as discussed in the next two sections.

6.2. Is the Sign Change in the Correlations Caused by the Different Emission Lines Used to Estimate M_{BH} ?

The opposite correlations for H β and C IV are intriguing but may represent problems with the broad line mass estimates. In particular, it is possible that the error in the broad line mass estimates is correlated with Γ_X , but in opposite ways for H β and C IV. The most likely source of such a spurious correlation would be a correlation between Γ_X and the scatter about the R - L relationship for H β and C IV, respectively. For example, if one were to systematically overestimate R with increasing Γ_X for the C IV emitting region, then one would infer a larger M_{BH} from C IV, and thus one would infer a spurious correlation between M_{BH} and Γ_X . However, the H β line

is only available at $z \lesssim 0.8$ and the C IV line is only available at $z \gtrsim 1.6$, and thus the change in sign for the Γ_X - M_{BH} correlations could be due to different spectral components shifting into or out of the observable X-ray spectral region (0.3–7.0 keV). In Figure 10, we show the distribution of M_{BH} as a function of z for the H β and C IV samples. As is clear from Figure 10, the C IV line is probing sources with $M_{BH} \gtrsim 3 \times 10^8 M_\odot$, while the H β line is probing sources with $M_{BH} \lesssim 3 \times 10^8 M_\odot$. Therefore, the change in sign for the Γ_X correlations could also be due to something more physically interesting, such as a change in the structure of the corona that occurs at some critical black hole mass or accretion rate.

We can test if the change in sign for the Γ_X correlations is the result of problems with the mass estimates for either H β or C IV, or if it is the result of the differences in z and M_{BH} probed by the two lines. While the Γ_X - M_{BH} relationship is weak compared to the Eddington ratio dependencies, we can use the Γ_X - M_{BH} relationship to test whether the non-monotonic dependency of Γ_X on Eddington ratio is a spurious result caused by systematic difference in the broad line mass estimates. This is because the Eddington ratios are inferred from the broad line mass estimates, and any systematic differences between the Eddington ratio inferred from H β as compared to C IV should also manifest themselves in the weaker Γ_X - M_{BH} relationship. This is true irregardless of whether the difference in slopes between the H β and C IV Γ_X - M_{BH} relationships is ‘statistically significant’ or not.

We compiled five sources from the literature at $z > 1.3$ with H β -based mass estimates of $M_{BH} > 5 \times 10^9 M_\odot$. In addition, we compiled five more sources from the literature at $z < 0.2$ and C IV-based mass estimates of $M_{BH} < 10^8 M_\odot$. This ‘test sample’ of 10 sources is listed in Table 2. Then, we test whether the H β test sources are better described by the H β regression or by the C IV regression, and likewise for the C IV test sources. If the change in sign for the Γ_X correlations is due to problems with the broad line mass estimates, then we would expect the H β -based mass estimates to be better described by the H β regression. However, if the change in sign is due to the difference in redshift and M_{BH} probed by the two regressions, then we would expect the H β test sources to be better described by the C IV regression, as the H β test sources are at high- z and have high- M_{BH} . A similar argument applies to the C IV test sources, since they are at low- z and have low black hole masses.

Figure 11 compares Γ_X and M_{BH} for H β and C IV for both the sources in our main sample and the test sources, as well as the best fit regression lines for the H β and C IV samples, respectively. The high- z , high- M_{BH} H β test sources appear to be better described by the high- z , high- M_{BH} C IV-based regression, and likewise the low- z , low- M_{BH} C IV test sources appear to be better described by the low- z , low- M_{BH} H β -based regression.

We can quantify this result by calculating the probability that the H β test sources ‘belong’ to the H β -based regression, as compared to the probability that the H β test sources ‘belong’ to the C IV-based regression. Assuming that the test sources are as equally likely to belong to either regression *a priori*, this ratio of probabilities is simply the ratio of the likelihood functions of the test sources for each regression relationship, where

the likelihood functions are given by Equation (24) in Kelly (2007); this ratio is called the ‘Bayes Factor’ (e.g., Congdon 2006). In order to incorporate our uncertainty in the regression parameters, we use the value of the likelihood function averaged over the probability distribution of the regression parameters. We find that the H β test sources are ≈ 250 times more likely to ‘belong’ to the C IV-based regression, and that the C IV test sources are ≈ 140 times more likely to ‘belong’ to the H β -based regression. Because the test sources are independent, it follows that the test sources are $\gtrsim 10^4$ times more likely to be described by the regression fit using the opposite emission line sample. This is further evidence that Γ_X and M_{BH} are not statistically independent; if Γ_X and M_{BH} were independent, then the test sources would not show a strong preference for either regression. Based on this analysis, we conclude that the change in sign of the Γ_X correlations is not due to problems associated with the use of the H β and C IV emission lines, but rather due to the different range of z and M_{BH} probed by the two subsamples.

6.3. Is the Sign Change in the Correlations Caused by the Different Redshift Ranges Probed?

While it appears that Γ_X has a nonmonotonic dependence on M_{BH} , L_{UV}/L_{Edd} , and L_X/L_{Edd} , it is unclear as to whether the sign change in the correlations is dependent on z or M_{BH} . However, we can test this in the same manner as was used to test if the sign change is due to problems with the H β - or C IV-based mass estimates. In this case, we need a sample of high- z , low- M_{BH} sources in order to break the degeneracy between M_{BH} and z . If the sign change in the correlation is redshift dependent, then we would expect the test sources to be better described by the high- z , high- M_{BH} C IV-based regression; but, if the sign change is black hole mass dependent, then we would expect the test sources to be better described by the low- z , low- M_{BH} H β -based regression.

Our test sample consists of nine $z > 1$, $\hat{M}_{BL} < 3 \times 10^8 M_\odot$ quasars from the Cosmic Evolution Survey (COSMOS, Scoville 2007), with optical spectra from Magellan (Trump et al. 2007) and X-ray spectra from XMM-Newton (Mainieri 2007). Black hole masses for these objects (Trump et al. 2008, in preparation) were estimated from the Mg II and C IV emission lines in the same manner as above. The objects are summarized in Table 3, and their location in the M_{BH} - z plane are shown in Figure 12. The COSMOS sources break the degeneracy between M_{BH} and z present in our SDSS sample, and are therefore adequate to test for a redshift dependence in the slope of the Γ_X - M_{BH} relationship. In Figure 13 we compare the COSMOS test sources with the H β - and C IV-based regressions. As can be seen, the high- z , low- M_{BH} COSMOS sources are better described by the low- z , low- M_{BH} regression. We can quantify this in the same manner as described in § 6.2 by averaging the likelihood function of the test sources over the posterior probability distribution. We find that the COSMOS test sources are $\gtrsim 10^5$ times more likely to be better described by the H β - Γ_X regression, and thus the sign change in the Γ_X correlations is not due to the difference in redshifts probed by the H β and C IV samples.

7. DISCUSSION

Previous work has found evidence for a correlation between α_{ox} and both M_{BH} (Brunner et al. 1997) and $L_{\text{bol}}/L_{\text{Edd}}$ (Wang et al. 2004), and for a correlation between Γ_X and both M_{BH} (e.g., Porquet et al. 2004; Piconcelli et al. 2005) and $L_{\text{bol}}/L_{\text{Edd}}$ (e.g., Lu & Yu 1999; Gierliński & Done 2004; Shemmer et al. 2006), in agreement with the results found in this work. However, our study differs from previous work in that we study a large sample of RQQs (318 sources with α_{ox} , 153 with Γ_X) over a broad range in black hole mass ($10^6 \lesssim M_{\text{BH}}/M_{\odot} \lesssim 10^{10}$) and redshift $0 < z < 4.8$; to date, this is the largest study of the dependence of the X-ray properties of RQQs on M_{BH} , $L_{\text{UV}}/L_{\text{Edd}}$, and L_X/L_{Edd} . In addition, this is the first study of its kind to correct for the intrinsic statistical uncertainty in broad line mass estimates when quantifying the *intrinsic* trends between the X-ray emission and M_{BH} , $L_{\text{UV}}/L_{\text{Edd}}$, and L_X/L_{Edd} .

Currently, there are two main types of geometries being considered for the comptonizing corona. The first of these is that of a ‘slab’-type geometry, possibly patchy, that sandwiches the disk (e.g., Bisnovatyi-Kogan & Blinnikov 1977; Galeev et al. 1979; Nayakshin 2000; Sobolewska et al. 2004b), and the second is that of a hot spherical inner advection dominated flow (e.g., Shapiro et al. 1976; Zdziarski et al. 1999); hybrids between the two geometries have also been considered (e.g., Poutanen et al. 1997; Sobolewska et al. 2004a). There is a growing body of evidence that the advection dominated hot inner flow does not exist in objects with Eddington ratios $L_{\text{bol}}/L_{\text{Edd}} \gtrsim 0.01$, as inferred from the existence of a relativistically broadened iron line (e.g., Mineo et al. 2000; Lee et al. 2002; Fabian et al. 2002), relativistically broadened reflection of ionized material (Janiuk et al. 2001), and by analogy with galactic black holes (e.g., Esin et al. 1997; Nowak et al. 2002). The range in Eddington ratios probed by our study is at most $0.03 \lesssim L_{\text{bol}}/L_{\text{Edd}} \lesssim 2$, with a mean of $L_{\text{bol}}/L_{\text{Edd}} \sim 0.25$. Therefore, the RQQs in our study are likely to have disks that extend approximately down to the last marginally stable orbit, and thus should only have the ‘slab’ type geometries.

7.1. Dependence of α_{ox} on M_{BH}

In this work we have found that RQQs become more X-ray quiet as M_{BH} increases, and confirmed the well-established relationship between α_{ox} and L_{UV} . Because L_{UV} increases with M_{BH} and the accretion rate relative to Eddington, \dot{m} , the well-known $\alpha_{\text{ox}}-L_{\text{UV}}$ correlation is likely driven by the $\alpha_{\text{ox}}-M_{\text{BH}}$ and $\alpha_{\text{ox}}-\dot{m}$ correlations. A correlation between α_{ox} and M_{BH} is expected even if the fraction of the bolometric luminosity emitted by the disk is independent of M_{BH} , as the effective temperature of the disk depends on M_{BH} . As M_{BH} increases, the effective temperature of the disk decreases, thus shifting the peak of the disk emission toward longer wavelengths. Because the flux density at 2500Å lies redward of the peak in the disk SED over most of the range M_{BH} probed by our study, this shift in the disk SED toward longer wavelengths produces an increase in L_{UV} relative to L_X .

We can use the standard thin disk solution to assess the evidence that the fraction of energy emitted by the corona depends on M_{BH} . We assume a simple model

where the spectrum for the disk emission is that expected for an extended thin accretion disk, and the spectrum for the corona emission is a simple power-law with exponential cutoffs at the low and high energy end. According to Wandel (2000), the spectrum from a radially extended thin accretion disk can be approximated as

$$f_{\nu}^D \approx A_D \left(\frac{\nu}{\nu_{\text{co}}} \right)^{-1/3} e^{-\nu/\nu_{\text{co}}}, \quad (23)$$

where A_D is the normalization and ν_{co} is the cut-off frequency. In this work, we choose the normalization to ensure that Equation (23) integrates to unity, and therefore f_{ν}^D gives the shape of the disk emission. For a Kerr black hole, Malkan (1991) finds that the cut-off frequency is related to M_{BH} as

$$h\nu_{\text{co}} = (6\text{eV})\dot{m}^{1/4}(M_{\text{BH}}/10^8 M_{\odot})^{-1/4}. \quad (24)$$

We assume that the X-ray emission from the corona can be described by a simple power law with an exponential cutoff at the high and low end:

$$f_{\nu}^C = A_C \nu^{-(\Gamma_X-1)} e^{-\nu/\nu_{\text{high}}} e^{-\nu_{\text{low}}/\nu}. \quad (25)$$

Here, A_C is the corona spectrum normalization, ν_{high} is the high energy cutoff, and ν_{low} is the low energy cutoff. We choose the low energy cutoff to be $\nu_{\text{low}} = 20$ eV, and we choose the high energy cutoff to be $\nu_{\text{high}} = 200$ keV (e.g., Gilli et al. 2007). As with Equation (23), we choose the normalization in Equation (25) to be equal to unity.

Denoting f_D to be the fraction of bolometric luminosity emitted by the disk, our model RQQ spectrum is then

$$L_{\nu} \approx L_{\text{bol}} [f_D f_{\nu}^D + (1 - f_D) f_{\nu}^C]. \quad (26)$$

We computed Equation (26) assuming a value of $\dot{m} = 0.2$ and $f_D = 0.85$. We chose the value of the $\dot{m} = 0.2$ because it is representative of the RQQs in our sample, and we chose the value $f_D = 0.85$ because it gives values of α_{ox} typical of the RQQs in our sample. We vary M_{BH} but keep f_D and \dot{m} constant because we are interested in investigating whether there is evidence that assuming independence between M_{BH} and both f_D and \dot{m} is inconsistent with our α_{ox} results.

We compute Equation (26) for two forms of the dependence of Γ_X on M_{BH} . For the first model, we assume a constant value of $\Gamma_X = 2$. For the second model, we assume that Γ_X depends on M_{BH} according to our best fit regression results, where Γ_X depends on M_{BH} according to Equation (12) for $M_{\text{BH}} \lesssim 3 \times 10^8 M_{\odot}$, and Γ_X depends on M_{BH} according to Equation (14) for $M_{\text{BH}} \gtrsim 3 \times 10^8 M_{\odot}$. We ignore the intrinsic dispersion in Γ_X . In Figure 14 we show the spectra computed from Equation (26) for RQQs with $M_{\text{BH}}/M_{\odot} = 10^7, 10^8, 10^9$, and 10^{10} . The dependence of the location of the peak in the disk emission on M_{BH} is clearly illustrated.

In Figure 15 we compare the $\alpha_{\text{ox}}-M_{\text{BH}}$ regression results with the dependence of α_{ox} on M_{BH} expected from Equation (26) for both Γ_X-M_{BH} models. Under the thin disk approximation, a correlation is expected between α_{ox} and M_{BH} , even if the fraction of bolometric luminosity emitted by the disk is independent of M_{BH} . However, our data are inconsistent with the assumption that f_D and M_{BH} are independent, given the thin disk approximation. Under the assumption that f_D and M_{BH} are

independent, the $\alpha_{\text{ox}}-M_{\text{BH}}$ correlation is too flat, and an increase in the fraction of bolometric luminosity emitted by the disk with increasing M_{BH} is needed to match the steeper observed dependence of α_{ox} on M_{BH} . Alternatively, if f_D increases with increasing \dot{m} , as we argue in § 7.2, then a steeper $\alpha_{\text{ox}}-M_{\text{BH}}$ correlation also results if M_{BH} and \dot{m} are correlated. In this case, if f_D increases with increasing \dot{m} , and if M_{BH} increases with increasing \dot{m} , then f_D will also increase with increasing M_{BH} , thus producing a steeper observed $\alpha_{\text{ox}}-M_{\text{BH}}$ correlation.

To the extent that Equations (23)–(26) accurately approximate the spectral shape of RQQs, our data imply that either the fraction of bolometric luminosity emitted by the disk increases with increasing M_{BH} , that M_{BH} and \dot{m} are correlated, or both. Some theoretical models have suggested that the fraction of bolometric luminosity emitted by the disk should depend on \dot{m} , but be relatively insensitive to M_{BH} (e.g., Czerny et al. 2003; Liu et al. 2003). Therefore, while a significant dependence of f_D on M_{BH} is not predicted by these disk/corona models, these models are still consistent with the interpretation that a $M_{\text{BH}}-\dot{m}$ correlation is driving the steeper $\alpha_{\text{ox}}-M_{\text{BH}}$ correlation. Unfortunately, without accurate estimates of \dot{m} we are unable to distinguish between these two possibilities.

A shift in the peak of the disk SED with M_{BH} may also explain the dependence of α_{ox} on redshift observed by K07. K07 speculated that the observed hardening of α_{ox} with increasing z at a given L_{UV} may be due to a correlation between α_{ox} and M_{BH} , manifested through a $M_{\text{BH}}-z$ correlation. At a given L_{UV} , an increase in M_{BH} will result in an increase in L_X relative to L_{UV} , assuming that \dot{m} is not strongly correlated with M_{BH} . This is because an increase in M_{BH} decreases the temperature of the disk, shifting the peak in the disk SED toward the red, and thus increasing the luminosity at 2500Å. However, since K07 investigated the dependence of α_{ox} on z at a given L_{UV} , the luminosity at 2500Å is held constant. Therefore, the overall disk emission must decrease in order to keep the luminosity at 2500Å constant despite the increase in M_{BH} . As a result, an increase in M_{BH} at a given L_{UV} will result in an increase in the X-ray luminosity relative to the luminosity at 2500Å. Because M_{BH} and z are correlated in our flux limited sample (e.g., see Figure 2), an increase in z will probe RQQs with higher M_{BH} . As a result, RQQs will become more X-ray loud with increasing z , at a given 2500Å luminosity. Consequently, deeper surveys that probe a greater range of M_{BH} should not see as strong of a correlation between M_{BH} and z , thereby reducing the magnitude of a $\alpha_{\text{ox}}-z$ correlation. Indeed, investigations based on samples that span a greater range in luminosity do not find evidence for a correlation between α_{ox} and z (e.g., Steffen et al. 2006; Just et al. 2007), qualitatively consistent with our interpretation of a $\alpha_{\text{ox}}-z$ correlation.

7.2. Dependence of α_{ox} on \dot{m}

We have found that α_{ox} increases with increasing $L_{\text{UV}}/L_{\text{Edd}}$, and decreases with increasing L_X/L_{Edd} . The mere existence of these correlations is not particularly interesting, as we would expect that the ratio of optical/UV luminosity to X-ray luminosity would increase as the fraction of optical/UV luminosity rela-

tive to Eddington increases, and vice versa for an increase in L_X/L_{Edd} . However, the relative magnitude of these dependencies carries some information regarding the dependence of α_{ox} on \dot{m} . A correlation between α_{ox} and $L_{\text{UV}}/L_{\text{Edd}}$ implies that L_{UV}/L_X increases as the quantity $f_{\text{UV}}\dot{m}$ increases, where f_{UV} is the fraction of bolometric luminosity emitted at 2500Å. Likewise, an anti-correlation between α_{ox} and L_X/L_{Edd} implies that L_{UV}/L_X decreases as the quantity $f_X\dot{m}$ increases, where f_X is the fraction of bolometric luminosity emitted at 2 keV. If the fraction of the bolometric luminosity emitted by the disk, as compared to the corona, increases with increasing \dot{m} , then we would expect a strong increase in L_{UV}/L_X with the product $f_{\text{UV}}\dot{m}$, resulting from the dual dependency of L_{UV}/L_X on f_{UV} and \dot{m} . Furthermore, because the fraction of bolometric luminosity emitted by the disk should decrease with increasing f_X , then, if the fraction of bolometric luminosity emitted by the disk increases with increasing \dot{m} , we would expect a weaker dependence of L_{UV}/L_X on the quantity $f_X\dot{m}$. This is because an increase in \dot{m} causes an increase in the disk emission relative to the corona emission, which will then work against the decrease in disk emission relative to the corona that results from an increase in f_X . The end result is a weaker dependence of L_{UV}/L_X on the product $f_X\dot{m}$. Indeed, this is what we observe, where $L_{\text{UV}}/L_X \propto (L_{\text{UV}}/L_{\text{Edd}})^{2.5}$ and $L_{\text{UV}}/L_X \propto (L_X/L_{\text{Edd}})^{-1.5}$. Therefore, we conclude that the disk emission relative to the corona emission increases with increasing \dot{m} . This is in agreement with some models of corona with a slab geometry (e.g., Czerny et al. 1997; Janiuk & Czerny 2000; Merloni & Fabian 2002; Liu et al. 2003), where the $\alpha_{\text{ox}}-\dot{m}$ correlation arises due to a dependency of the size of the corona on \dot{m} .

Our result that α_{ox} is correlated with $L_{\text{UV}}/L_{\text{Edd}}$ and anti-correlated with L_X/L_{Edd} is inconsistent with a constant bolometric correction to both the optical/UV and X-ray luminosities. Instead, an increase in L_{UV}/L_X with increasing \dot{m} implies that the bolometric correction depends on \dot{m} . Because we conclude that the fraction of bolometric luminosity emitted by the disk increases with increasing \dot{m} , this implies that the bolometric correction to the optical/UV luminosity decreases with increasing \dot{m} , while the bolometric correction to the X-ray luminosity increases with increasing \dot{m} . The direction of this trend is consistent with the results of Vasudevan & Fabian (2007), who find that the bolometric correction to the X-ray luminosity increases with increasing $L_{\text{bol}}/L_{\text{Edd}}$. Similarly, we have found evidence that the fraction of bolometric luminosity emitted by the disk depends on M_{BH} , therefore implying that the bolometric correction also depends on M_{BH} . Even if the fraction of bolometric luminosity emitted by the disk is independent of M_{BH} , the bolometric correction will still depend on M_{BH} because the location of the peak in the disk emission will shift toward longer wavelengths as M_{BH} increases. As M_{BH} varies, the luminosity at 2500Å probes a different region of the quasi-blackbody disk emission, thereby producing a dependence of bolometric correction on M_{BH} .

7.3. Implications for Black Hole Feedback

A significant amount of recent work suggests that radiative and mechanical feedback energy from AGN plays an important part in galaxy and supermassive black hole coevolution (e.g., Fabian 1999; Wyithe & Loeb 2003; Hopkins et al. 2005). Within the context of these models, a nuclear inflow of gas, possibly the result of a galaxy merger, feeds the SMBH, thus igniting a quasar. The SMBH grows until feedback energy from the quasar is able to drive out the accreting gas, thus halting the accretion process. Hydrodynamic calculations of accretion flows have shown that the efficiency of the quasar in driving an outflow depends on the fraction of energy emitted through the UV/disk component as compared to the X-ray/corona component (Proga 2007). The disk component produces luminosity in the UV, which is responsible for driving an outflow via radiation pressure on lines, whereas the corona component produces luminosity in the X-rays, which is responsible for driving an outflow via thermal expansion. Calculations by Proga (2007) have shown that radiation driving produces an outflow that carries more mass and energy than thermal driving. If the efficiency of black hole feedback depends on the quasar SED, any dependence on M_{BH} and \dot{m} of the fraction of AGN energy emitted in the UV as compared to the X-ray has important consequences for models of black hole growth.

Because we have found evidence that the fraction of bolometric luminosity emitted by the disk increases with increasing \dot{m} and M_{BH} , this implies that black holes become more efficient at driving an outflow with increasing \dot{m} and M_{BH} . However, the α_{ox} - M_{BH} correlation may be due to the combination of both a correlation between M_{BH} and \dot{m} , and a dependence of the location peak in the disk SED on M_{BH} . If the fraction of energy emitted by the disk only depends weakly on M_{BH} , as some theoretical models have suggested (e.g., Czerny et al. 2003; Liu et al. 2003), the fraction of energy emitted in the UV will still decrease with increasing M_{BH} because the peak of the disk emission will shift away from the UV. In this case, at a given \dot{m} we would expect that black holes will become less efficient at driving an outflow with increasing M_{BH} .

7.4. Dependence of Γ_X on M_{BH} and \dot{m}

In this work we have also found evidence that Γ_X and M_{BH} , L_{UV}/L_{Edd} , and L_X/L_{Edd} are not statistically independent. Moreover, the dependence of Γ_X on black hole mass or Eddington ratio appears to follow a non-monotonic form, although the Γ_X - M_{BH} trend is weak compared to the dependency of Γ_X on Eddington ratio. For the Γ_X - M_{BH} relationship, the X-ray continuum hardens with increasing black hole mass until $M_{BH} \sim 3 \times 10^8 M_\odot$, after which the X-ray continuum softens with increasing black hole mass. The opposite is true for the Γ_X - L_{UV}/L_{Edd} and Γ_X - L_X/L_{Edd} trends, and further work is needed to confirm this result. Previous studies have not seen this non-monotonic trend because they have only employed the H β emission line, and therefore their samples have been dominated by low- z , low- M_{BH} sources.

7.4.1. Selection Effects

It is unlikely that the dependence of Γ_X on M_{BH} , L_{UV}/L_{Edd} , or L_X/L_{Edd} is due to redshifting of

the observable spectra range. If this were the case, then as M_{BH} increases, so does z due to selection effects, and thus we would observe a decrease in Γ_X as the ‘soft excess’ shifts out of the observed 0.3–7 keV spectral range, while the compton reflection component shifts into the observed spectral range. However, there are lines of evidence that suggest that the Γ_X correlation are not due to redshifting of the observable spectral region, and that at least some of the observed dependency of Γ_X on M_{BH} , L_{UV}/L_{Edd} , and L_X/L_{Edd} is real. First, in § 6.3 we tested whether a sample of nine $z > 1$ test sources with $M_{BH} \lesssim 3 \times 10^8 M_\odot$ were better described by a regression fit using the $z > 1.5$, $M_{BH} \gtrsim 3 \times 10^8 M_\odot$ sources, or by a regression fit using the $z < 1$, $M_{BH} \lesssim 3 \times 10^8 M_\odot$ sources. We found that the test sources were better fit using the regression of similar M_{BH} , and therefore that the difference in the Γ_X - M_{BH} correlations primarily depends on M_{BH} . Second, similar trends at low redshift between Γ_X and M_{BH} or L_{bol}/L_{Edd} have been seen in other studies that only analyze the hard X-ray spectral slope (typically 2–12 keV, e.g., Piconcelli et al. 2005; Shemmer et al. 2006), and thus these studies are not effected by the soft excess. Third, the compton reflection hump is unlikely to shift into the observable spectral range until $z \sim 1$. However, the contribution to the inferred Γ_X from compton reflection at $z \gtrsim 1$ is likely weak, if not negligible, as our $z \gtrsim 1$ sources have $M_{BH} \gtrsim 10^8 M_\odot$ and are highly luminous, and therefore are expected to only have weak reflection components (Mineo et al. 2000; Ballantyne et al. 2001; Bianchi et al. 2007).

There are two scenarios in which the non-monotonic behavior of Γ_X with M_{BH} or Eddington ratio may be artificially caused by selection. We will focus on the Eddington ratio dependency, as it is the strongest; however, our argument also applies to M_{BH} . First, the intrinsic dependency of Γ_X on Eddington ratio could be linear with increasing intrinsic scatter at high L_{bol}/L_{Edd} . Then, an inferred non-monotonic trend would occur if we were to systematically miss quasars with high L_{bol}/L_{Edd} and steep X-ray spectra. Alternatively, there could be no intrinsic dependency of Γ_X on Eddington ratio. In this case, we would infer a non-monotonic trend if we were to systematically miss quasars with steep X-ray spectra at low and high L_{bol}/L_{Edd} , and quasars with flat X-ray spectra at moderate L_{bol}/L_{Edd} .

We do not consider it likely that the observed non-monotonic dependence of Γ_X on Eddington ratio is due solely to selection effects. K07 describes the sample selection for sources with Γ_X . With the exception of some of the $z > 4$ quasars, all sources from K07 were selected by cross-correlating the SDSS DR3 quasars with public *Chandra* observations. Almost all SDSS sources in K07 had serendipitous *Chandra* observations, and therefore were selected without regard to their X-ray properties. K07 estimated Γ_X for all sources that were detected in X-rays at the level of 3σ or higher. Therefore, the only additional criterion beyond the SDSS selection imposed by K07 is the requirement that the source had to be detected in X-ray, which was fulfilled by 90% of the quasars; the undetected sources were slightly more likely to be found at lower redshift, probably due to the presence of unidentified BAL quasars. As a result, the K07 sample selection function is essentially equivalent to the

SDSS quasar selection function. Because the SDSS selects quasars based on their optical colors, the most likely cause of selection effects is the optical color selection. There is evidence that Γ_X is correlated with the slope of the optical continuum, where the X-ray continuum flattens (hardens) as the optical continuum steepens (softens) (Gallagher et al. 2005, K07). The SDSS selection probability is lower for red sources (Richards et al. 2006), so we might expect to systematically miss sources with smaller Γ_X . However, for the two scenarios described above, this is opposite the trend needed to explain the Γ_X - L_X/L_{Edd} relationship, where we need to at least systematically miss sources with larger Γ_X . Furthermore, the drop in SDSS selection efficiency with optical spectral slope only occurs at $2 < z < 4$ (Richards et al. 2006), thus we would expect a redshift dependence of this selection effect. As we have argued above, and in § 6.3, the non-monotonic trends for Γ_X cannot be completely explained as the result of different redshift ranges being probed.

7.4.2. Implications for Accretion Physics

The dependence of Γ_X on L_{UV}/L_{Edd} and L_X/L_{Edd} is likely due to a dependence of Γ_X on \dot{m} . If these Γ_X correlations were due to a dependence of Γ_X on f_{UV} or f_X , then we would expect opposite trends for L_{UV}/L_{Edd} and L_X/L_{Edd} , as f_{UV} and f_X should be anti-correlated. The fact that the regression results for the Γ_X - L_{UV}/L_{Edd} and Γ_X - L_X/L_{Edd} relationships are similar implies that Γ_X depends on \dot{m} , and at most only weakly on f_{UV} or f_X .

A non-monotonic dependence of Γ_X on \dot{m} is predicted from the accreting corona model of Janiuk & Czerny (2000), as well as a non-monotonic dependence of Γ_X on the viscosity (Bechtold et al. 2003). In addition, Γ_X is expected to steepen with increasing optical depth (e.g., Haardt & Maraschi 1991, 1993; Czerny et al. 2003). One could then speculate that the dependence of Γ_X on M_{BH} or \dot{m} is due to a non-monotonic dependence of the corona optical depth on \dot{m} , which may indicate a change in the structure of the disk/corona system at $\sim 3 \times 10^8 M_\odot$ or some critical \dot{m} . Recent work also suggests a non-monotonic dependence of the optical/UV spectral slope, α_{UV} , on \dot{m} (Bonning et al. 2007; Davis et al. 2007). From this work, it has been inferred that the optical/UV continuum becomes more red with increasing \dot{m} until $L_{bol}/L_{Edd} \approx 0.3$, after which the optical/UV continuum becomes more blue with increasing \dot{m} . Assuming the bolometric corrections described in § 4.2, the turnover in the Γ_X - L_{bol}/L_{Edd} relationship also occurs at $L_{bol}/L_{Edd} \approx 0.3$. Bonning et al. (2007) suggested that the turnover in spectral slope at $L_{bol}/L_{Edd} \sim 0.3$ may be due to a change in accretion disk structure, where the inner part of the accretion disk becomes thicker due to increased radiation pressure (Abramowicz et al. 1988). Bonning et al. (2007) performed a simple approximation to this ‘slim disk’ solution and found that it is able to produce a non-monotonic trend between optical color and Eddington ratio. If the inner disk structure changes at high \dot{m} , this change could alter the corona structure, producing the observed trend between Γ_X and Eddington ratio.

Unfortunately, current models for corona geometry make a number of simplifying assumptions, and do not

yet predict a specific relationship between α_{ox} , Γ_X , M_{BH} , and \dot{m} . Ideally, full magneto-hydrodynamic simulations (e.g., De Villiers et al. 2003; Turner 2004; Krolik et al. 2005) that include accretion disk winds (e.g., Murray et al. 1995; Proga & Kallman 2004) should be used to interpret the results found in this work. However, MHD simulations have not advanced to the point where they predict the dependence of α_{ox} and Γ_X on quasar fundamental parameters, but hopefully recent progress in analytical descriptions of the magneto-rotational instability (Pessah et al. 2006, 2007) will help to overcome some of the computational difficulties and facilitate further advancement.

8. SUMMARY

In this work we have investigated the dependence of α_{ox} and Γ_X on black hole mass and Eddington ratio using a sample of 318 radio-quiet quasars with X-ray data from *ROSAT* (Strateva et al. 2005) and *Chandra* (Kelly et al. 2007), and optical data mostly from the SDSS; 153 of these sources have estimates of Γ_X from *Chandra*. Our sample spans a broad range in black hole mass ($10^6 \lesssim M_{BH}/M_\odot \lesssim 10^{10}$), redshift ($0 < z < 4.8$), and luminosity ($10^{43} \lesssim \lambda L_\lambda(2500\text{\AA})[\text{erg s}^{-1}] \lesssim 10^{48}$). To date, this is the largest study of the dependence of RQQ X-ray parameters on M_{BH} , L_{UV}/L_{Edd} , and L_X/L_{Edd} . Our main results are summarized as follows:

- We show that α_{ox} is correlated with L_{UV}/L_{Edd} and anti-correlated with L_X/L_{Edd} . This result is inconsistent with a constant bolometric correction being applicable to both the optical/UV luminosity and the X-ray luminosity. This result, when taken in combination with recent work by Vasudevan & Fabian (2007), implies that constant bolometric corrections can be considerably unreliable and lead to biased results. Instead, we argue that L_{UV}/L_X increases with increasing \dot{m} and increasing M_{BH} , therefore implying that the bolometric correction depends on \dot{m} and M_{BH} .
- We performed a linear regression of α_{ox} on luminosity, black hole mass, L_{UV}/L_{Edd} , and L_X/L_{Edd} , and found significant evidence that α_{ox} depends on all four quantities: $L_{UV}/L_X \propto L_{UV}^{0.31 \pm 0.03}$, $L_{UV}/L_X \propto M_{BH}^{0.43 \pm 0.06}$, $L_{UV}/L_X \propto (L_{UV}/L_{Edd})^{2.57 \pm 0.45}$, and $L_{UV}/L_X \propto L_X/L_{Edd}^{-1.48 \pm 0.14}$. The dependence of α_{ox} on L_{UV} may be due to the dual dependence of α_{ox} on M_{BH} and \dot{m} . Because we have attempted to correct for the statistical uncertainties in α_{ox} and the broad line estimates of M_{BH} , these results refer to the *intrinsic* relationships involving α_{ox} and M_{BH} , and are not merely the relationships between α_{ox} and the broad line mass estimates, $\hat{M}_{BL} \propto L^\gamma FWHM^2$.
- A correlation between α_{ox} and M_{BH} is expected from the fact that the peak in the disk emission will shift to longer wavelengths as M_{BH} increases, even if the fraction of the bolometric luminosity emitted by the disk does not change with M_{BH} . Using a simple model for RQQ spectra, we argue that the observed α_{ox} - M_{BH} correlation is steeper than that

expected if both \dot{m} and the fraction of bolometric luminosity produced by the disk are independent of M_{BH} . The observed $\alpha_{ox}-M_{BH}$ relationship therefore implies that either the fraction of bolometric luminosity emitted by the disk increases with increasing M_{BH} , that M_{BH} is correlated with \dot{m} , or both.

- A correlation between α_{ox} and \dot{m} is predicted from several models of ‘slab’-type corona. We argue that the weaker dependence of α_{ox} on L_X/L_{Edd} implies that L_{UV}/L_X increases with increasing \dot{m} . Considering that the efficiency of quasar feedback energy in driving an outflow may depend on the ratio of UV to X-ray luminosity, a correlation between α_{ox} and both M_{BH} and \dot{m} has important consequences for models of black hole growth. In particular, if supermassive black holes become more X-ray quiet at higher \dot{m} , they will become more efficient at driving away their accreting gas, thus halting their growth.
- Because of a possible nonlinear dependence of Γ_X on M_{BH} , L_{UV}/L_{Edd} , or L_X/L_{Edd} , we performed separate regressions for the black hole mass estimates obtained from each emission line. We confirmed the significant dependence of Γ_X on L_{UV}/L_{Edd} and L_X/L_{Edd} seen in previous studies as inferred from the broad line mass estimates based on the H β line; however, we also find evidence that the Γ_X correlations change direction when including the C IV line. In particular, for the H β sample, the X-ray continuum hardens with increasing M_{BH} , while for the C IV sample, the X-ray continuum softens with increasing M_{BH} . Similar but opposite trends are seen with respect to L_{UV}/L_{Edd} and L_X/L_{Edd} , and we conclude that these relationships can be interpreted as resulting from a correlation between Γ_X and \dot{m} . Results obtained from the Mg II line were too uncertain to interpret. We analyzed two test samples to argue that this non-monotonic behavior is not due to the different redshifts probed by the two samples, or to

problems with the estimates of M_{BH} derived from the two lines; the different trends may be due to the difference in M_{BH} probed by the two samples. A non-monotonic dependence of Γ_X on M_{BH} and/or \dot{m} may imply a change in the disk/corona structure, although a non-monotonic dependence of Γ_X on \dot{m} and the viscosity is predicted by some models of ‘slab’-type coronal geometries.

We would like to thank the anonymous referee for a careful reading and comments that contributed to the improvement of this paper. This research was funded in part by NSF grant AST03-07384, NASA contract NAS8-39073, and Chandra Award Number G05-6113X issued by the Chandra X-ray Observatory Center. Funding for the SDSS and SDSS-II has been provided by the Alfred P. Sloan Foundation, the Participating Institutions, the National Science Foundation, the U.S. Department of Energy, the National Aeronautics and Space Administration, the Japanese Monbukagakusho, the Max Planck Society, and the Higher Education Funding Council for England. The SDSS Web Site is <http://www.sdss.org/>.

The SDSS is managed by the Astrophysical Research Consortium for the Participating Institutions. The Participating Institutions are the American Museum of Natural History, Astrophysical Institute Potsdam, University of Basel, University of Cambridge, Case Western Reserve University, University of Chicago, Drexel University, Fermilab, the Institute for Advanced Study, the Japan Participation Group, Johns Hopkins University, the Joint Institute for Nuclear Astrophysics, the Kavli Institute for Particle Astrophysics and Cosmology, the Korean Scientist Group, the Chinese Academy of Sciences (LAMOST), Los Alamos National Laboratory, the Max-Planck-Institute for Astronomy (MPIA), the Max-Planck-Institute for Astrophysics (MPA), New Mexico State University, Ohio State University, University of Pittsburgh, University of Portsmouth, Princeton University, the United States Naval Observatory, and the University of Washington.

REFERENCES

- Abramowicz, M. A., Czerny, B., Lasota, J. P., & Szuszkiewicz, E. 1988, *ApJ*, 332, 646
- Akritas, M. G., & Bereshady, M. A. 1996, *ApJ*, 470, 706
- Anderson, S. F., et al. 2001, *AJ*, 122, 503
- Avni, Y., & Tananbaum, H. 1982, *ApJ*, 262, L17
- Ballantyne, D. R., Ross, R. R., & Fabian, A. C. 2001, *MNRAS*, 327, 10
- Bechtold, J., et al. 2003, *ApJ*, 588, 119
- Begelman, M. C., & Nath, B. B. 2005, *MNRAS*, 361, 1387
- Bentz, M. C., Peterson, B. M., Pogge, R. W., Vestergaard, M., & Onken, C. A. 2006, *ApJ*, 644, 133
- Bian, W.-H. 2005, *Chinese Journal of Astronomy and Astrophysics Supplement*, 5, 289
- Bianchi, S., Guainazzi, M., Matt, G., & Fonseca Bonilla, N. 2007, *A&A*, 467, L19
- Bisnovatyi-Kogan, G. S., & Blinnikov, S. I. 1977, *A&A*, 59, 111
- Boller, T., Brandt, W. N., & Fink, H. 1996, *A&A*, 305, 53
- Bonning, E. W., Cheng, L., Shields, G. A., Salvander, S., & Gebhardt, K. 2007, *ApJ*, 659, 211
- Brandt, W. N., Mathur, S., & Elvis, M. 1997, *MNRAS*, 285, L25
- Brandt, N., & Boller, T. 1998, *Astronomische Nachrichten*, 319, 163
- Brocksopp, C., Starling, R. L. C., Schady, P., Mason, K. O., Romero-Colmenero, E., & Puchnarewicz, E. M. 2006, *MNRAS*, 366, 953
- Bromley, J. M., Somerville, R. S., & Fabian, A. C. 2004, *MNRAS*, 350, 456
- Brunner, H., Mueller, C., Friedrich, P., Doerrer, T., Staubert, R., & Riffert, H. 1997, *A&A*, 326, 885
- Budavári, T., et al. 2005, *ApJ*, 619, L31
- Cardelli, J. A., Clayton, G. C., & Mathis, J. S. 1989, *ApJ*, 345, 245
- Collin, S., Kawaguchi, T., Peterson, B. M., & Vestergaard, M. 2006, *A&A*, 456, 75
- Congdon, P. 2006, *Bayesian Statistical Modelling* (2nd. Ed.; West Sussex: John Wiley & Sons Ltd.)
- Constantin, A., Shields, J. C., Hamann, F., Foltz, C. B., & Chaffee, F. H. 2002, *ApJ*, 565, 50
- Czerny, B., Nikolajuk, M., Rózańska, A., Dumont, A.-M., Loska, Z., & Zycki, P. T. 2003, *A&A*, 412, 317
- Czerny, B., Witt, H. J., & Zycki, P. 1997, *The Transparent Universe*, 382, 397
- Dai, X., Chartas, G., Eracleous, M., & Garmire, G. P. 2004, *ApJ*, 605, 45
- Davis, S. W., Woo, J.-H., & Blaes, O. M. 2007, *ApJ*, 668, 682
- Dempster, A., Laird, N., & Rubin, D. 1977, *J. R. Statist. Soc. B.*, 39, 1
- De Villiers, J.-P., Hawley, J. F., & Krolik, J. H. 2003, *ApJ*, 599, 1238
- Di Matteo, T., Springel, V., & Hernquist, L. 2005, *Nature*, 433, 604
- Elvis, M., Risaliti, G., & Zamorani, G. 2002, *ApJ*, 565, L75
- Elvis, M., et al. 1994, *ApJS*, 95, 1
- Esin, A. A., McClintock, J. E., & Narayan, R. 1997, *ApJ*, 489, 865
- Fabian, A. C. 1999, *MNRAS*, 308, L39
- Fabian, A. C., et al. 2002, *MNRAS*, 335, L1

- Fox, J. 1997, *Applied Regression Analysis, Linear Models, and Related Methods* (Thousand Oaks: Sage Publications, Inc.)
- Fuller, W. A. 1987, *Measurement Error Models* (New York: John Wiley & Sons)
- Galeev, A. A., Rosner, R., & Vaiana, G. S. 1979, *ApJ*, 229, 318
- Gallagher, S. C., Brandt, W. N., Chartas, G., & Garmire, G. P. 2002, *ApJ*, 567, 37
- Gallagher, S. C., Richards, G. T., Hall, P. B., Brandt, W. N., Schneider, D. P., & Vanden Berk, D. E. 2005, *AJ*, 129, 567
- Gallagher, S. C., Brandt, W. N., Chartas, G., Priddey, R., Garmire, G. P., & Sambruna, R. M. 2006, *ApJ*, 644, 709
- Gebhardt, K., et al. 2000, *ApJ*, 539, L13
- Gierliński, M., & Done, C. 2004, *MNRAS*, 349, L7
- Gilli, R., Comastri, A., & Hasinger, G. 2007, *A&A*, 463, 79
- Green, P. J., Aldcroft, T. L., Mathur, S., Wilkes, B. J., & Elvis, M. 2001, *ApJ*, 558, 109
- Grupe, D., Mathur, S., Wilkes, B., & Osmer, P. 2006, *AJ*, 131, 55
- Grupe, D., Thomas, H.-C., & Beuermann, K. 2001, *A&A*, 367, 470
- Haardt, F., & Maraschi, L. 1991, *ApJ*, 380, L51
- Haardt, F., & Maraschi, L. 1993, *ApJ*, 413, 507
- Hastie, T., Tibshirani, R., & Friedman, J. 2001, *The Elements of Statistical Learning* (New York: Springer-Verlag)
- Hatziminaoglou, E., Mathez, G., Solanes, J.-M., Manrique, A., & Salvador-Solé, E. 2003, *MNRAS*, 343, 692
- Hopkins, P. F., Hernquist, L., Cox, T. J., Di Matteo, T., Martini, P., Robertson, B., & Springel, V. 2005, *ApJ*, 630, 705
- Hopkins, P. F., Hernquist, L., Cox, T. J., Di Matteo, T., Robertson, B., & Springel, V. 2006, *ApJS*, 163, 1
- Hopkins, P. F., Richards, G. T., & Hernquist, L. 2007, *ApJ*, 654, 731
- Janiuk, A., & Czerny, B. 2000, *New Astronomy*, 5, 7
- Janiuk, A., Czerny, B., & Madejski, G. M. 2001, *ApJ*, 557, 408
- Just, D. W., Brandt, W. N., Shemmer, O., Steffen, A. T., Schneider, D. P., Chartas, G., & Garmire, G. P. 2007, *ApJ*, 665, 1004
- Kaspi, S., Maoz, D., Netzer, H., Peterson, B. M., Vestergaard, M., & Jannuzi, B. T. 2005, *ApJ*, 629, 61
- Kauffmann, G., & Haehnelt, M. 2000, *MNRAS*, 311, 576
- Kelly, B. C. 2007, *ApJ*, 665, 1489
- Kelly, B. C., & Bechtold, J. 2007, *ApJS*, 168, 1
- Kelly, B. C., Bechtold, J., Siemiginowska, A., Aldcroft, T., & Sobolewska, M. 2007, *ApJ*, 657, 116 (K07)
- Kollmeier, J. A., et al. 2006, *ApJ*, 648, 128
- Krolik, J. H. 2001, *ApJ*, 551, 72
- Krolik, J. H., Hawley, J. F., & Hirose, S. 2005, *ApJ*, 622, 1008
- Laor, A., Fiore, F., Elvis, M., Wilkes, B. J., & McDowell, J. C. 1997, *ApJ*, 477, 93
- Lee, J. C., Iwasawa, K., Houck, J. C., Fabian, A. C., Marshall, H. L., & Canizares, C. R. 2002, *ApJ*, 570, L47
- Liang, E. P. T., & Price, R. H. 1977, *ApJ*, 218, 247
- Liu, B. F., Mineshige, S., & Ohsuga, K. 2003, *ApJ*, 587, 571
- Lu, Y., & Yu, Q. 1999, *ApJ*, 526, L5
- Mainieri, V. 2007, in press at *ApJS* (astro-ph/0612361)
- Malkan, M. 1991, *IAU Colloq. 129: The 6th Institute d'Astrophysique de Paris (IAP) Meeting: Structure and Emission Properties of Accretion Disks*, 165
- Markowitz, A., Edelson, R., & Vaughan, S. 2003, *ApJ*, 598, 935
- Mathur, S. 2000, *MNRAS*, 314, L17
- McIntosh, D. H., Rieke, M. J., Rix, H.-W., Foltz, C. B., & Weymann, R. J. 1999, *ApJ*, 514, 40
- McLure, R. J., & Dunlop, J. S. 2004, *MNRAS*, 352, 1390
- McLure, R. J., & Jarvis, M. J. 2002, *MNRAS*, 337, 109
- Merloni, A., & Fabian, A. C. 2002, *MNRAS*, 332, 165
- Merritt, D., & Ferrarese, L. 2001, *ApJ*, 547, 140
- Mineo, T., et al. 2000, *A&A*, 359, 471
- Murray, N., Chiang, J., Grossman, S. A., & Voit, G. M. 1995, *ApJ*, 451, 498
- Nandra, K., George, I. M., Mushotzky, R. F., Turner, T. J., & Yaqoob, T. 1997, *ApJ*, 477, 602
- Nayakshin, S. 2000, *ApJ*, 534, 718
- Nishihara, E., Yamashita, T., Yoshida, M., Watanabe, E., Okumura, S.-I., Mori, A., & Iye, M. 1997, *ApJ*, 488, L27
- Nowak, M. A., Wilms, J., & Dove, J. B. 2002, *MNRAS*, 332, 856
- O'Neill, P. M., Nandra, K., Papadakis, I. E., & Turner, T. J. 2005, *MNRAS*, 358, 1405
- Onken, C. A., Ferrarese, L., Merritt, D., Peterson, B. M., Pogge, R. W., Vestergaard, M., & Wandel, A. 2004, *ApJ*, 615, 645
- Page, K. L., Reeves, J. N., O'Brien, P. T., Turner, M. J. L., & Worrall, D. M. 2004, *MNRAS*, 353, 133
- Page, K. L., Turner, M. J. L., Reeves, J. N., O'Brien, P. T., & Sembay, S. 2003, *MNRAS*, 338, 1004
- Péroux, C., Storrie-Lombardi, L. J., McMahon, R. G., Irwin, M., & Hook, I. M. 2001, *AJ*, 121, 1799
- Pessah, M. E., Chan, C.-K., & Psaltis, D. 2006, *MNRAS*, 372, 183
- Pessah, M. E., Chan, C.-k., & Psaltis, D. 2007, in press at *ApJ*(arXiv:0705.0352)
- Peterson, B. M., et al. 2004, *ApJ*, 613, 682
- Piconcelli, E., Jimenez-Bailón, E., Guainazzi, M., Schartel, N., Rodríguez-Pascual, P. M., & Santos-Lleo, M. 2005, *A&A*, 432, 15
- Porquet, D., Reeves, J. N., O'Brien, P., & Brinkmann, W. 2004, *A&A*, 422, 85
- Poutanen, J., Krolik, J. H., & Ryde, F. 1997, *MNRAS*, 292, L21
- Proga, D. 2005, *ApJ*, 630, L9
- Proga, D. 2007, *ApJ*, 661, 693
- Proga, D., & Kallman, T. R. 2004, *ApJ*, 616, 688
- Reeves, J. N., & Turner, M. J. L. 2000, *MNRAS*, 316, 234
- Reeves, J. N., Turner, M. J. L., Ohashi, T., & Kii, T. 1997, *MNRAS*, 292, 468
- Reichard, T. A., et al. 2003, *AJ*, 126, 2594
- Richards, G. T., et al. 2006, *AJ*, 131, 2766
- Risaliti, G., & Elvis, M. 2005, *ApJ*, 629, L17
- Schlegel, D. J., Finkbeiner, D. P., & Davis, M. 1998, *ApJ*, 500, 525
- Schneider, D. P., et al. 2005, *AJ*, 130, 376
- Schwartz, G. 1979, *Ann. Statist.*, 6, 461
- Scoville, N. Z., et al. 2007, in press at *ApJS*(astro-ph/0612305)
- Shakura, N. I., & Syunyaev, R. A. 1973, *A&A*, 24, 337
- Shapiro, S. L., Lightman, A. P., & Eardley, D. M. 1976, *ApJ*, 204, 187
- Shemmer, O., Brandt, W. N., Netzer, H., Maiolino, R., & Kaspi, S. 2006, *ApJ*, 646, L29
- Silk, J., & Rees, M. J. 1998, *A&A*, 331, L1
- Sobolewska, M. A., Siemiginowska, A., & Życki, P. T. 2004a, *ApJ*, 608, 80
- Sobolewska, M. A., Siemiginowska, A., & Życki, P. T. 2004b, *ApJ*, 617, 102
- Spergel, D. N., et al. 2003, *ApJS*, 148, 175
- Springel, V., Di Matteo, T., & Hernquist, L. 2005, *ApJ*, 620, L79
- Stapleton, D. C. & Young, D. J. 1984, *Econometrica*, 52, 737
- Steffen, A. T., Strateva, I., Brandt, W. N., Alexander, D. M., Koekemoer, A. M., Lehmer, B. D., Schneider, D. P., & Vignali, C. 2006, *AJ*, 131, 2826
- Storrie-Lombardi, L. J., McMahon, R. G., Irwin, M. J., & Hazard, C. 1996, *ApJ*, 468, 121
- Strateva, I. V., Brandt, W. N., Schneider, D. P., Vanden Berk, D. G., & Vignali, C. 2005, *AJ*, 130, 387 (S05)
- Tananbaum, H., et al. 1979, *ApJ*, 234, L9
- Turner, N. J. 2004, *ApJ*, 605, L45
- Tremaine, S., et al. 2002, *ApJ*, 574, 740
- Trump, J. R., et al. 2006, *ApJS*, 165, 1
- Trump, J., Impey, C., et al. 2007, in press at *ApJS*(astro-ph/0606016)
- Trump, J., Impey, C., et al. 2008, in preparation
- Uttley, P., McHardy, I. M., & Papadakis, I. E. 2002, *MNRAS*, 332, 231
- Vasudevan, R. V., & Fabian, A. C. 2007, in press at *MNRAS*, (arXiv:0708.4308)
- Véron-Cetty, M.-P., Joly, M., & Véron, P. 2004, *A&A*, 417, 515
- Vestergaard, M. 2002, *ApJ*, 571, 733
- Vestergaard, M. 2004, *ApJ*, 601, 676
- Vestergaard, M., et al. 2007, in preparation
- Vestergaard, M., & Peterson, B. M. 2006, *ApJ*, 641, 689
- Vestergaard, M., & Wilkes, B. J. 2001, *ApJS*, 134, 1
- Vignali, C., Brandt, W. N., Fan, X., Gunn, J. E., Kaspi, S., Schneider, D. P., & Strauss, M. A. 2001, *AJ*, 122, 2143
- Vignali, C., Brandt, W. N., Schneider, D. P., Garmire, G. P., & Kaspi, S. 2003, *AJ*, 125, 418
- Vignali, C., Brandt, W. N., & Schneider, D. P. 2003, *AJ*, 125, 433
- Vignali, C., Brandt, W. N., Schneider, D. P., & Kaspi, S. 2005, *AJ*, 129, 2519
- Vignali, C., Comastri, A., Cappi, M., Palumbo, G. G. C., Matsuoka, M., & Kubo, H. 1999, *ApJ*, 516, 582
- Wandel, A. 2000, *New Astronomy Review*, 44, 427
- Wandel, A., Peterson, B. M., & Malkan, M. A. 1999, *ApJ*, 526, 579
- Wang, J.-M., Watarai, K.-Y., & Mineshige, S. 2004, *ApJ*, 607, L107
- Wilkes, B. J., & Elvis, M. 1987, *ApJ*, 323, 243
- Wilkes, B. J., Tananbaum, H., Worrall, D. M., Avni, Y., Oey, M. S., & Flanagan, J. 1994, *ApJS*, 92, 53
- Woo, J., & Urry, C. M. 2002, *ApJ*, 579, 530
- Worrall, D. M., Tananbaum, H., Giommi, P., & Zamorani, G. 1987, *ApJ*, 313, 596
- Wyithe, J. S. B., & Loeb, A. 2003, *ApJ*, 595, 614
- Yuan, W., Siebert, J., & Brinkmann, W. 1998b, *A&A*, 334, 498
- Zamorani, G., et al. 1981, *ApJ*, 245, 357
- Zdziarski, A. A., Lubinski, P., & Smith, D. A. 1999, *MNRAS*, 303, L11

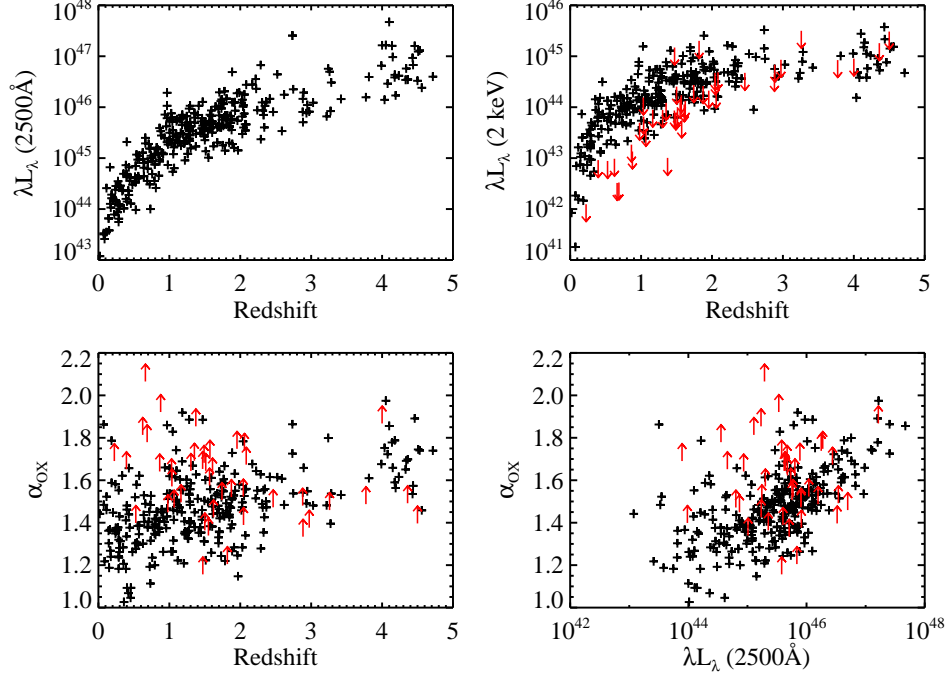


FIG. 1.— The (L_{UV}, L_X, z) distribution of our sample. Non-detections are denoted by red arrows.

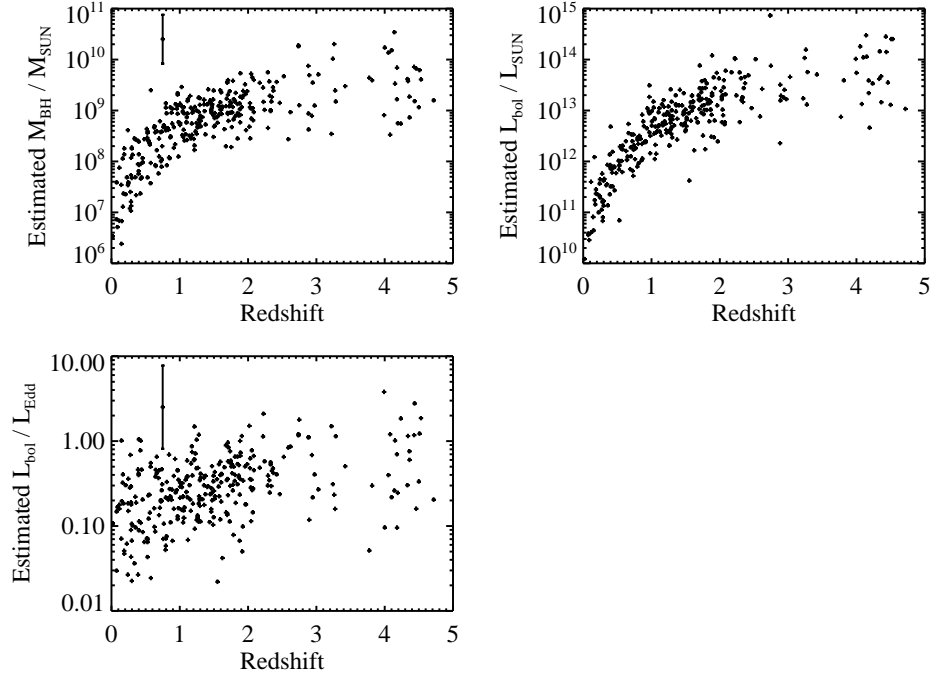


FIG. 2.— The distributions of estimated M_{BH} , L_{bol} , and L_{bol}/L_{Edd} , as a function of z for our sample. The data points with error bars in the left two plots are fictitious data points illustrating the typical error in \hat{M}_{BL} and $\hat{L}_{bol}/\hat{L}_{Edd}$.

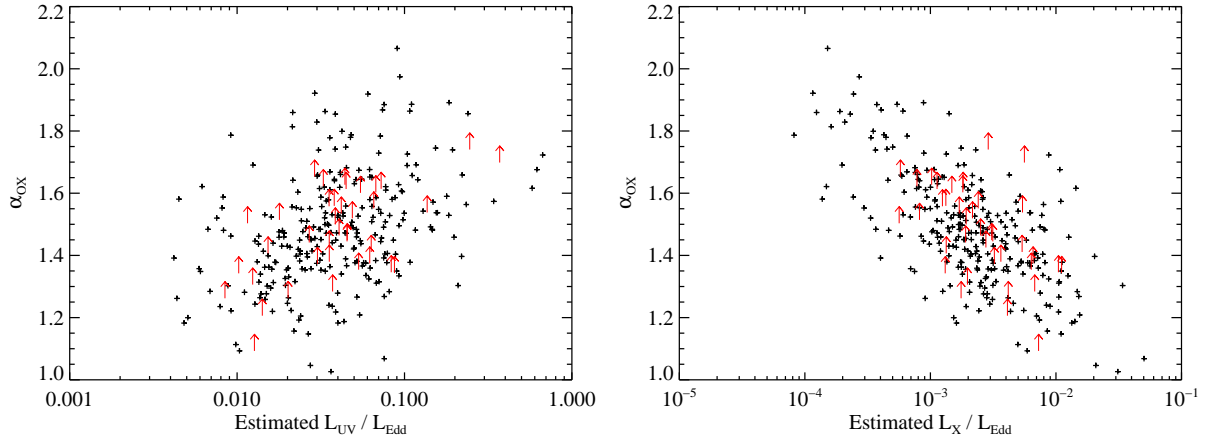


FIG. 3.— The distribution of α_{ox} as a function of $L_{\text{UV}}/L_{\text{Edd}}$ (left) and $L_{\text{X}}/L_{\text{Edd}}$ (right). The opposite dependence of α_{ox} on $L_{\text{UV}}/L_{\text{Edd}}$ and $L_{\text{X}}/L_{\text{Edd}}$ suggests that at least one of these quantities is not proportional to $L_{\text{bol}}/L_{\text{Edd}}$. As such, we do not employ bolometric corrections in this work, and instead compare directly with $L_{\text{UV}}/L_{\text{Edd}}$ and $L_{\text{X}}/L_{\text{Edd}}$.

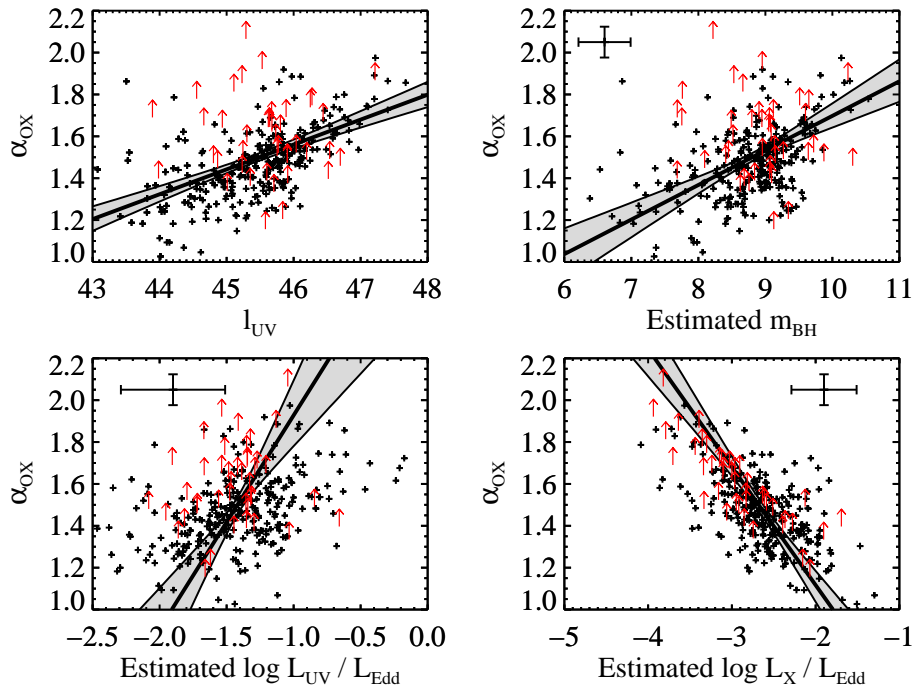


FIG. 4.— Ratio of optical/UV to X-ray flux as a function of L_{UV} , M_{BH} , $L_{\text{UV}}/L_{\text{Edd}}$, and $L_{\text{X}}/L_{\text{Edd}}$. The solid lines denote the best fit, and the shaded regions contain 95% (2σ) of the probability on the regression line. The data points with error bars in the plots of α_{ox} as a function of M_{BH} , $L_{\text{UV}}/L_{\text{Edd}}$, and $L_{\text{X}}/L_{\text{Edd}}$ are fictitious and illustrate the typical errors in each direction.

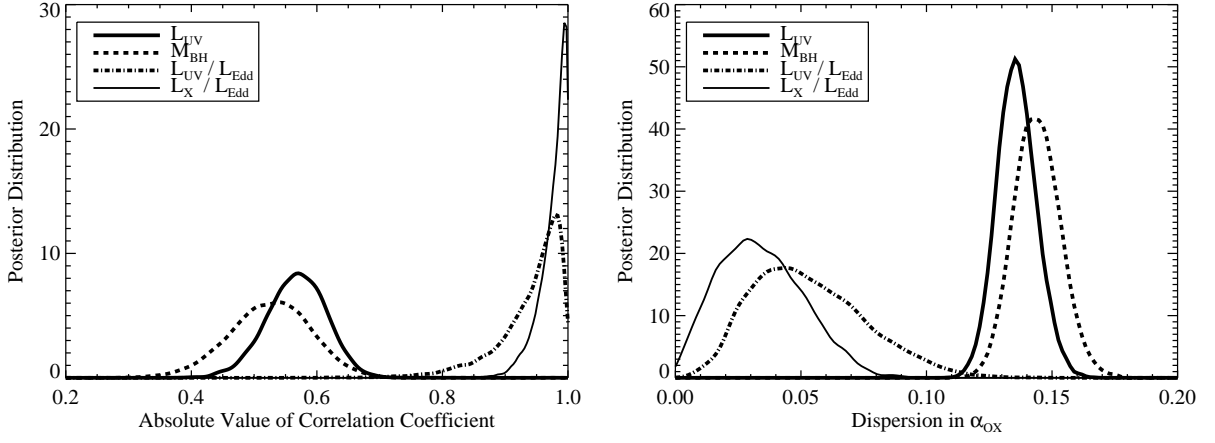


FIG. 5.— Posterior probability distributions for the absolute value of the correlation coefficients between α_{ox} and $\log L_{UV}$, $\log M_{BH}$, $\log L_{UV}/L_{Edd}$, and $\log L_X/L_{Edd}$ (left) and for the intrinsic dispersion in α_{ox} at a given L_{UV} , M_{BH} , L_{UV}/L_{Edd} , or L_X/L_{Edd} (right). The thick solid line denotes the probability distribution for the two quantities with respect to L_{UV} , the dashed line for the two quantities with respect to M_{BH} , the dashed-dotted line for the two quantities with respect to L_{UV}/L_{Edd} , and the thin solid line for the two quantities with respect to L_X/L_{Edd} .

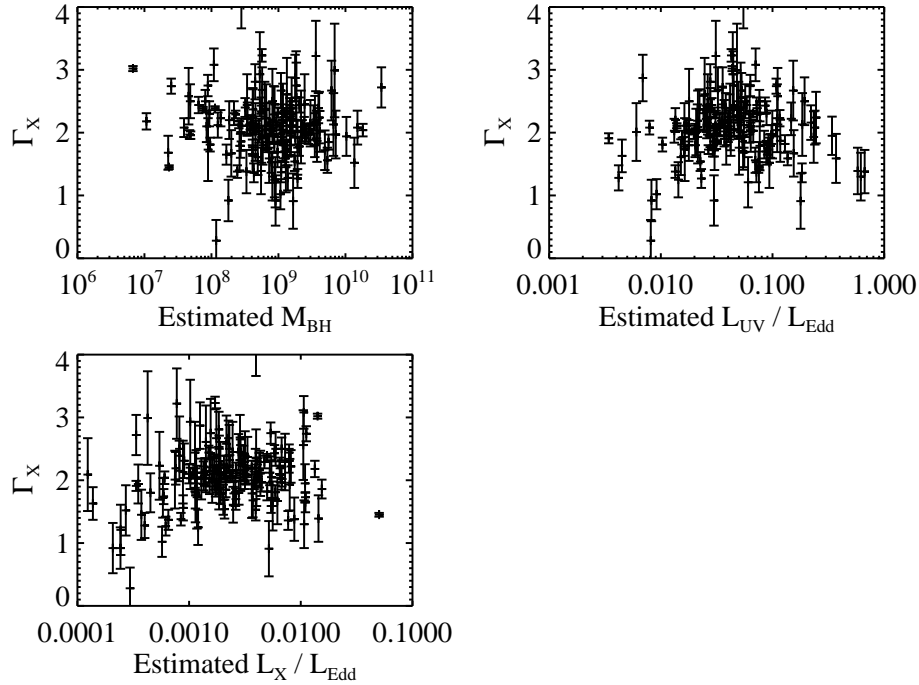


FIG. 6.— Distribution of the X-ray photon index as a function of estimated M_{BH} , L_{UV}/L_{Edd} , and L_X/L_{Edd} . For clarity, error bars are only shown on Γ_X , and we cut-off the one data point with estimated $\Gamma_X > 4$. While no obvious trends between Γ_X and M_{BH} , L_{UV}/L_{Edd} , or L_X/L_{Edd} exist for the whole sample, there is evidence of opposite trends in Γ_X for the H β and C IV samples.

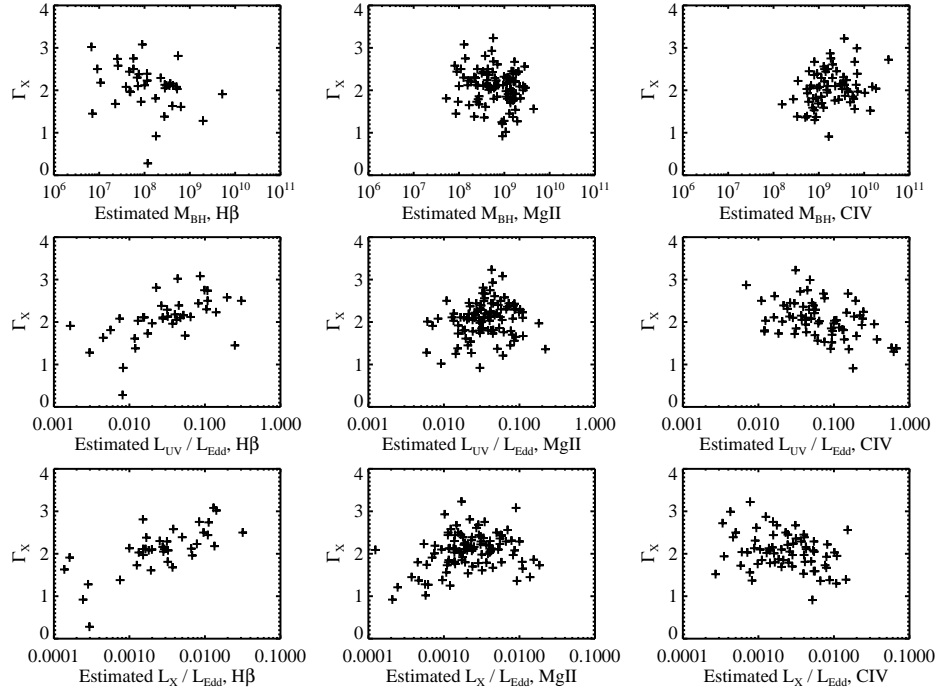


FIG. 7.— Distribution of the X-ray photon index as a function of estimated M_{BH} , L_{UV}/L_{Edd} , and L_X/L_{Edd} for the individual emission lines. For clarity, error bars have been omitted, and we omit the one data point with estimated $\Gamma_X > 4$. While no obvious trends exist for the whole sample, there is evidence of opposite trends for the H β and C IV samples.

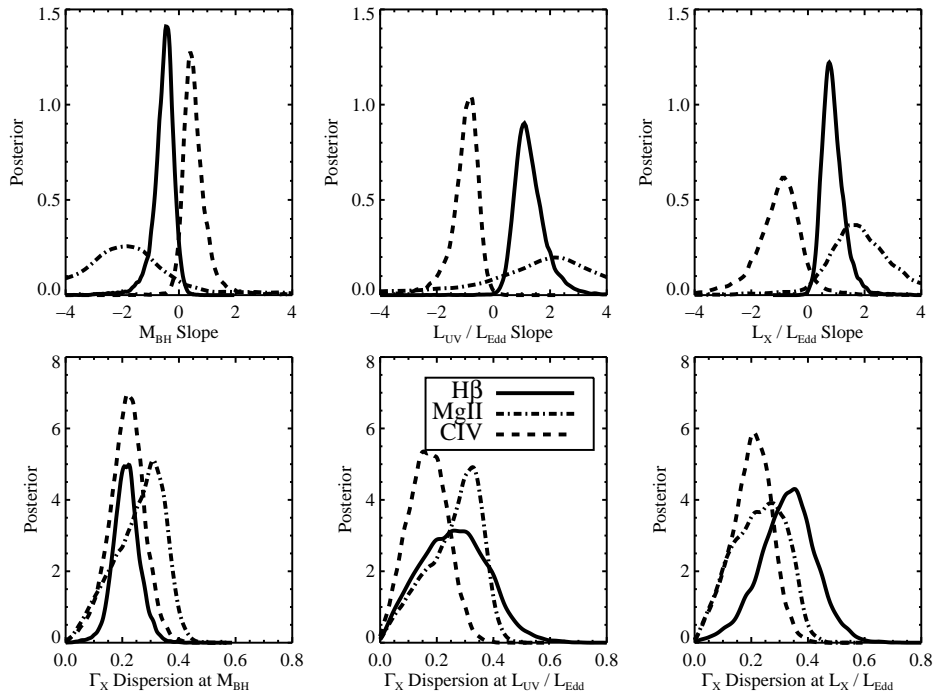


FIG. 8.— Posterior probability distributions of the slope (top) and intrinsic dispersion (bottom) from a linear regression of Γ_X on $\log M_{BH}$, $\log L_{UV}/L_{Edd}$, and $\log L_X/L_{Edd}$. The solid lines mark the posterior for the regression using the H β sample, the dashed-dotted lines mark the posterior for the regression using the Mg II sample, and the dashed lines mark the posterior for the regression using the C IV sample.

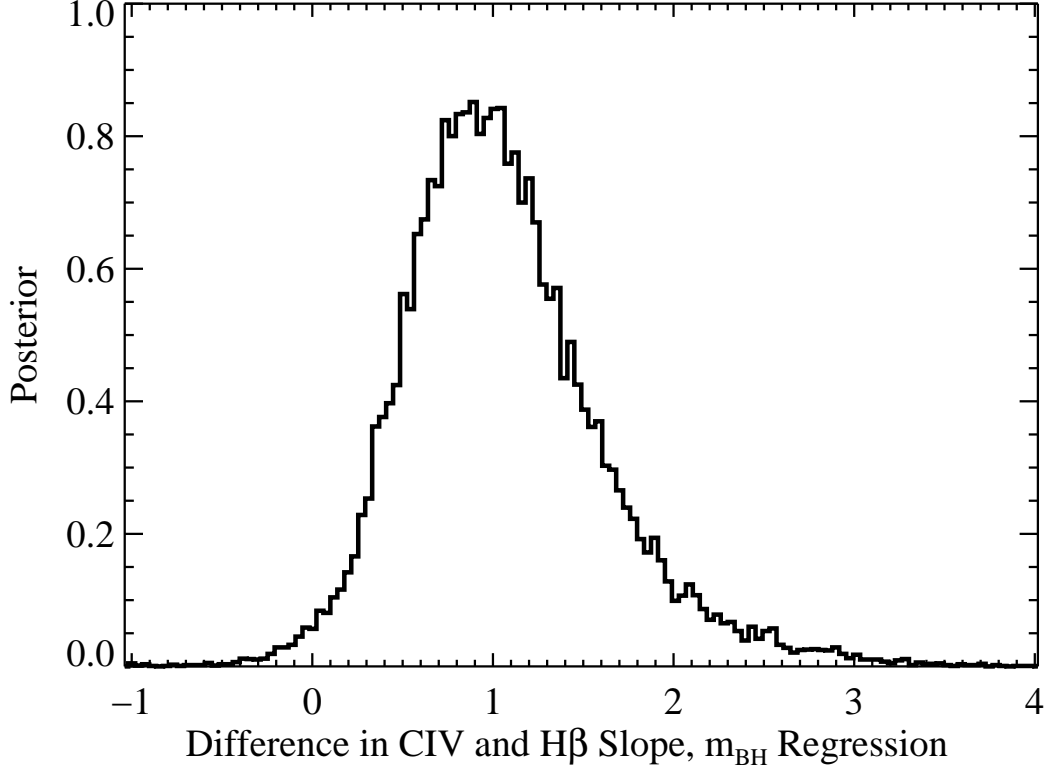


FIG. 9.— Posterior distribution for the difference in slopes between the C IV and H β regressions of Γ_X on m_{BH} . While there is no significant evidence that either the H β or C IV regression slope is different from zero, there *is* significant evidence that they are not the same, implying a nonmonotonic trend between Γ_X and M_{BH} .

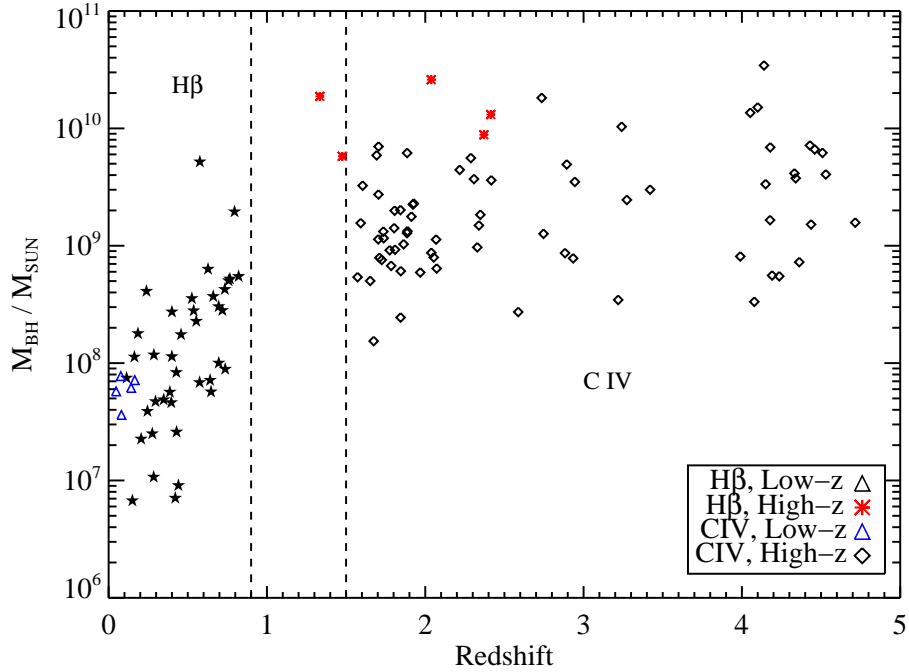


FIG. 10.— Distribution of estimated M_{BH} as a function of z for the H β sample (stars) and the C IV sample (open diamonds). The H β sample probes sources with lower M_{BH} and z , while the C IV sample probes sources with higher M_{BH} and z . To break the degeneracy between emission line, M_{BH} , and z , we have collected a sample of H β test sources (red asterisks) at high M_{BH} and z , and a sample of C IV test sources (open blue triangles) at low M_{BH} and z .

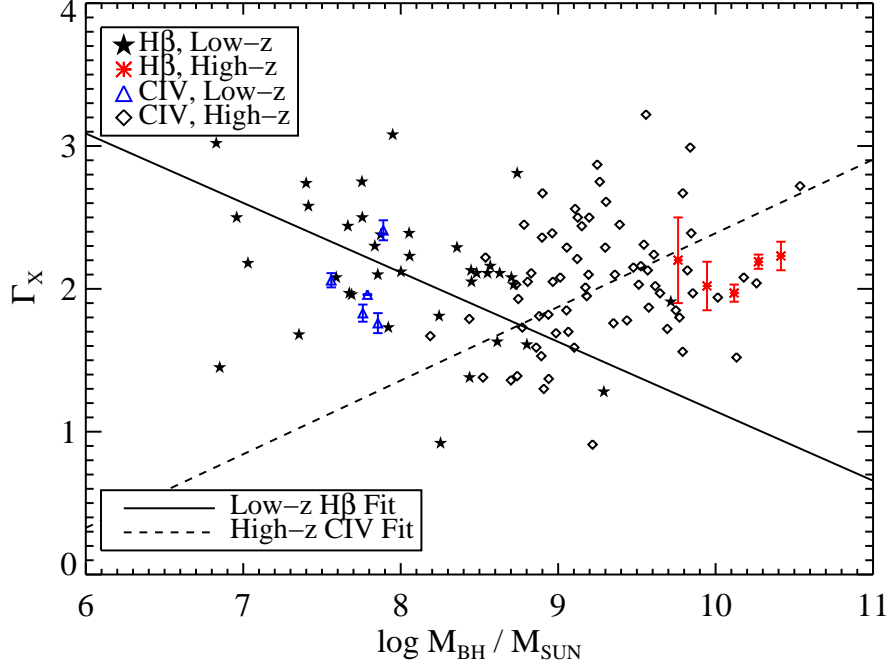


FIG. 11.— X-ray photon index as a function of estimated M_{BH} for low- z sources with M_{BH} derived from the $H\beta$ line, high- z test sources with M_{BH} derived from the $H\beta$ line, low- z test sources with M_{BH} derived from the C IV line, and high- z sources with M_{BH} derived from the C IV line. The symbols are the same as in Figure 10. Also shown is the best fit regression using the $H\beta$ sample (solid line) and the C IV sample (dashed line). The high- z $H\beta$ sources are better described by the high- z C IV regression, and the low- z C IV sources are better described by the low- z $H\beta$ regression, implying that the difference in slopes between the $H\beta$ and C IV samples is not due to systematic differences in mass estimates derived from either line.

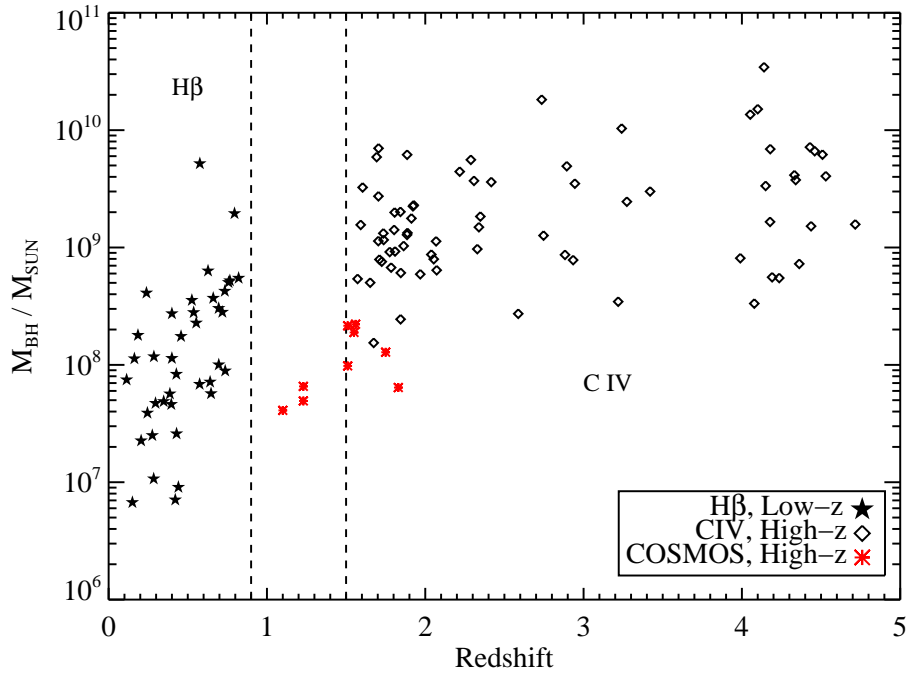


FIG. 12.— Same as Figure 10, but for the lower M_{BH} and higher z test sources from COSMOS. These test sources help break the degeneracy between the M_{BH} and z present in our main sample.

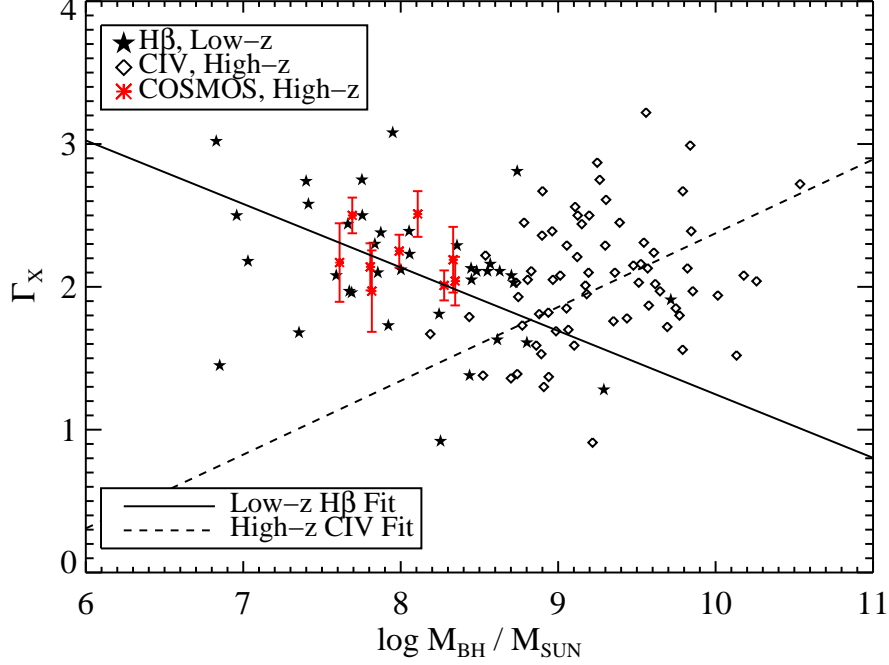


FIG. 13.— Same as Figure 11, but for a sample of high- z , low- M_{BH} test sources from *COSMOS* (red asterisks with error bars). The *COSMOS* sources are better described by the low- z , low- M_{BH} regression, implying that the difference in slopes between the $H\beta$ and C IV samples is due to the difference in M_{BH} probed by the two samples, and not due to the redshift differences.

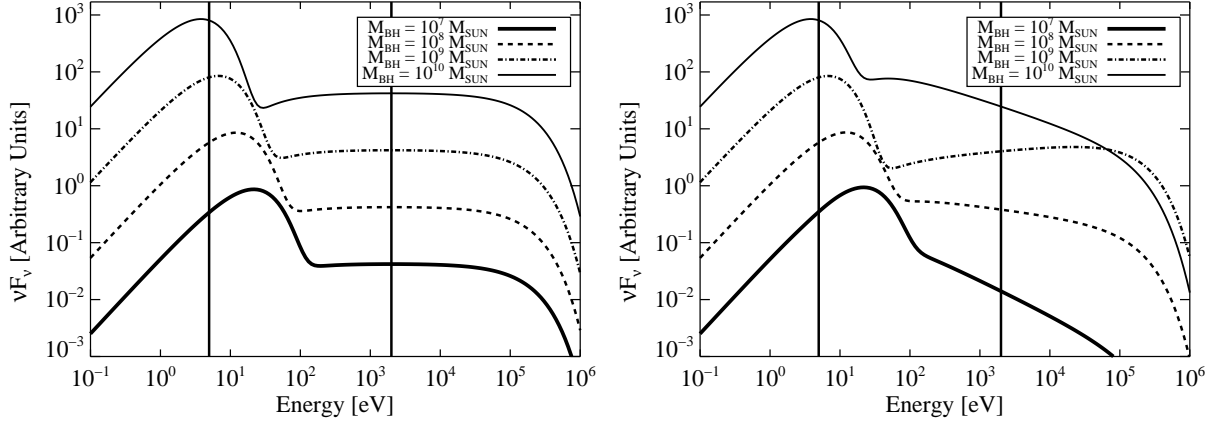


FIG. 14.— Model RQQ spectra computed from Equations (23)–(26), assuming $\Gamma_X = 2$ (left) and a varying Γ_X with M_{BH} (right). The spectra are computed for a RQQ with $M_{BH}/M_\odot = 10^7$ (thick solid line), 10^8 (dashed line), 10^9 (dashed-dotted line), and 10^{10} (thin solid line). In all cases we assume $\dot{m} = 0.2$ and that $f_D = 85\%$ of the bolometric luminosity is emitted by the disk. The vertical lines mark the locations of 2500\AA and 2 keV . The dependence of the location of the peak in the disk emission on M_{BH} is apparent, producing a correlation between α_{ox} and M_{BH} even if the fraction of bolometric luminosity emitted by the disk is independent of M_{BH} .

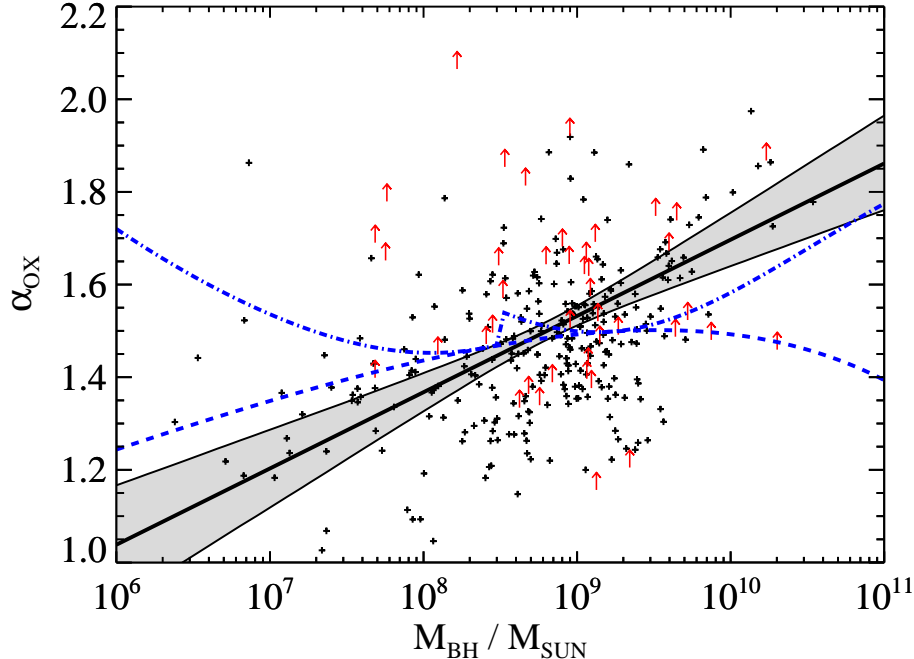


FIG. 15.— Dependence of α_{ox} on M_{BH} computed from Equations (23)–(26), assuming $\Gamma_X = 2$ (blue dashed line) and a varying Γ_X with M_{BH} (blue dot-dashed line). As with Figure 14, we compute Equations (23)–(26) assuming $\dot{m} = 0.2$ and $f_D = 0.85$. The predictions from the model RQQ spectra are compared with our observed data and the regression results, where the symbols and lines have the same meaning as in Figure 4. The $\alpha_{\text{ox}}-M_{\text{BH}}$ relationships predicted from assuming that f_D is independent of M_{BH} are inconsistent with the observed $\alpha_{\text{ox}}-M_{\text{BH}}$ relationship.

TABLE 1
BLACK HOLE PARAMETERS OF THE SAMPLE

α (J2000)	δ (J2000)	z	$\log \hat{M}_{\text{BL}}/M_{\odot}$	$\log L_X/\hat{L}_{\text{Edd}}^{\text{a}}$	$\log L_{\text{UV}}/\hat{L}_{\text{Edd}}^{\text{b}}$
00 02 30.7	+00 49 59.0	1.352	9.20 ± 0.45	-2.43 ± 0.45	-1.44 ± 0.45
00 06 54.1	-00 15 33.4	1.725	9.08 ± 0.29	-2.58 ± 0.30	-1.07 ± 0.29
00 22 10.0	+00 16 29.3	0.574	7.96 ± 0.32	-2.73 ± 0.32	-1.11 ± 0.32
00 27 52.4	+00 26 15.7	0.205	7.35 ± 0.45	-2.42 ± 0.46	-1.26 ± 0.49
00 31 31.4	+00 34 20.2	1.735	9.17 ± 0.29	-2.66 ± 0.29	-1.31 ± 0.29
00 50 06.3	-00 53 19.0	4.331	9.61 ± 0.41	-2.89 ± 0.42	-1.19 ± 0.41
00 57 01.1	+14 50 03.0	0.623	8.66 ± 0.32	-3.79 ± 0.32	-1.66 ± 0.32
00 59 22.8	+00 03 01.0	4.178	9.21 ± 0.38	-2.28 ± 0.41	-0.74 ± 0.38
01 06 19.2	+00 48 22.0	4.437	9.18 ± 0.38	-1.96 ± 0.39	-0.46 ± 0.38
01 13 05.7	+15 31 46.5	0.576	9.39 ± 0.32	-3.47 ± 0.32	-2.46 ± 0.32
01 13 09.1	+15 35 53.6	1.806	9.19 ± 0.29	-2.32 ± 0.29	-1.13 ± 0.29
01 15 37.7	+00 20 28.7	1.275	9.25 ± 0.45	-2.75 ± 0.45	-1.81 ± 0.45
01 26 02.2	-00 19 24.1	1.765	8.96 ± 0.29	-2.58 ± 0.29	-1.01 ± 0.29

NOTE. — The complete version of this table is in the electronic edition of the Journal. The printed edition contains only a sample.

^a Logarithm of the ratio of νL_{ν} [2 keV] to \hat{L}_{Edd} , where \hat{L}_{Edd} is calculated from the broad emission line estimate of $M_{\text{BH}}, \hat{M}_{\text{BL}}$.

^b Logarithm of the ratio of νL_{ν} [2500Å] to \hat{L}_{Edd} , where \hat{L}_{Edd} is calculated from the broad emission line estimate of $M_{\text{BH}}, \hat{M}_{\text{BL}}$.

TABLE 2
SOURCES WITH H β AND C IV USED FOR TESTING THE Γ_X - M_{BH} CORRELATIONS

Quasar Name	α (J2000)	δ (J2000)	z	Line	$\log \hat{M}_{BL}$ M_{\odot}	$\hat{L}_{bol}/\hat{L}_{Edd}$	Opt. Ref. ^a	Γ_X	X-ray Ref. ^b
PG 0026+129	00 29 13.7	+13 16 03.8	0.142	C IV	7.789	1.768	1	1.96 ^c	5
Fairall 9	01 23 45.7	-58 48 21.8	0.046	C IV	7.760	0.265	1	1.83 ± 0.06	6
PG 1202+281	12 04 42.2	+27 54 12.0	0.165	C IV	7.855	0.359	1	1.76 ± 0.07	7
PG 1211+143	12 14 17.7	+14 03 12.3	0.080	C IV	7.559	1.380	1	2.06 ± 0.05	8
PG 1247+267	12 50 05.7	+26 31 07.7	2.038	H β	10.41	0.379	2	2.23 ± 0.10	9
Q1346-036	13 48 44.1	-03 53 25.0	2.370	H β	9.946	0.609	3	2.02 ± 0.17	3
MRK 478	14 42 07.5	+35 26 22.9	0.077	C IV	7.890	0.498	1	2.41 ± 0.07	7
PG 1630+377	16 32 01.1	+37 37 50.0	1.476	H β	9.762	0.569	4	2.20 ± 0.30	10
PG 1634+706	16 34 28.9	+70 31 33.0	1.334	H β	10.27	0.734	4	2.19 ± 0.05	10
HE 2217-2818	22 20 06.8	-28 03 23.9	2.414	H β	10.12	0.807	3	1.97 ± 0.06	3

REFERENCES. — (1) Kelly & Bechtold (2007) (2) McIntosh et al. (1999) (3) Shemmer et al. (2006) (4) Nishihara et al. (1997) (5) O’Neill et al. (2005) (6) Nandra et al. (1997) (7) Brocksopp et al. (2006) (8) Reeves & Turner (2000) (9) Page et al. (2004) (10) Piconcelli et al. (2005)

^a Reference for the rest frame optical/UV data.

^b Reference for the X-ray data.

^c O’Neill et al. (2005) do not report an error on Γ_X .

TABLE 3
TEST SOURCES FROM COSMOS

α (J2000)	δ (J2000)	z	Line	$\log \hat{M}_{BL}$ M_{\odot}	$\hat{L}_{bol}/\hat{L}_{Edd}$	Γ_X
09 58 48.8	+02 34 42.3	1.551	C IV	8.276	0.131	2.01 ± 0.11
09 59 02.6	+02 25 11.8	1.105	Mg II	7.612	0.025	2.17 ± 0.28
09 59 49.4	+02 01 41.1	1.758	C IV	8.108	0.719	2.51 ± 0.16
10 00 50.0	+02 05 00.0	1.235	Mg II	7.692	0.501	2.50 ± 0.13
10 00 51.6	+02 12 15.8	1.829	Mg II	7.807	0.131	2.14 ± 0.17
10 00 58.9	+01 53 59.5	1.559	C IV	8.346	0.172	2.04 ± 0.17
10 02 19.6	+01 55 36.9	1.509	C IV	8.333	0.177	2.19 ± 0.23
10 02 34.4	+01 50 11.5	1.506	C IV	7.991	0.941	2.25 ± 0.12
10 02 43.9	+02 05 02.0	1.234	Mg II	7.817	0.303	1.97 ± 0.29